INDIA IN THE PROTEROZOIC: TWO KEY SPATIAL AND TEMPORAL CONSTRAINTS

By

LAURA C. GREGORY

A THESIS PRESENTED TO THE GRADUATE SCHOOL
OF THE UNIVERSITY OF FLORIDA IN PARTIAL FULFILLMENT
OF THE REQUIREMENTS FOR THE DEGREE OF
MASTER OF SCIENCE

UNIVERSITY OF FLORIDA

2008

To my Dad, who consistently encourages my enthusiasm for science and the natural world.

ACKNOWLEDGMENTS

I would like to thank the members of my committee, Joe Meert, David Foster, and Neil Opdyke, for consistently guiding me through this research and offering fantastic advice and critical review. I especially want to thank Joe for encouraging creative scientific thinking and teaching me so many interesting things. I thank my parents, Christine and William, and my sister, Amanda, for all of their help along the way. My dad really taught me the joy of science from day one and learning has always been a crucial part of my life because of my parents. I want to thank all of my closest friends in geology- we have really been through everything together, from the very beginning of undergraduate geology into competent scientists with the highest ambitions. Alexa van Eaton deserves special thanks for her constant encouragement and unrelenting enthusiasm. I thank Emily Grudem, Laura Ruhl, Elodie Bourbon, Braden Fitzgerald, and Jessica Yff. I also want to thank Misty Stroud for being my enthusiastic sounding board and partner in tectonic geology.

There are some very crucial people that contitributed significantly to the science involved in this research- in lab training, analyses, field work, and scientific discussion and review. They are Vimal Pradhan, Shawn Malone, James Vogl, George Kamenov, Bernard Bingen, Trond Torsvik, Dan Gorman, Endale Tamrat, Kainian Huang, Linda Sohl, Dhiraj Banerjee, Bob Tucker, and Alan Collins. M. Whitehouse is thanked for operating the NORDSIM laboratory and controlling quality of U-Pb data.

I want to thank the Geological Sciences faculty for guiding me for the past five years and teaching me vast amounts of geology. I especially thank James Vogl and Ray Russo for their contribution. Finally, I thank my best friends throughout the past few years who have always lended a seemingly interested ear to my enthusiasm for science, and with whom I have had some of the greatest experiences- Amber Beutler, Nicole Yutulis, and Annie Reynolds.

Funding for this research was provided by the National Science Foundation grant EAR04-0901 to Joseph Meert, and the Universityof Florida University Scholars Program grant.

TABLE OF CONTENTS

LIST OF TABLES

LIST OF FIGURES

LIST OF ABBREVIATIONS

2σ	two sigma units (expression of error)
α_{95}	circle of 95% confidence about the mean
AF	alternating field
$^{40}Ar/^{39}Ar$	ratio of argon isotopes 40 and 39
˚C	degrees Celcius
ca.	circa
ChRc	characteristic remanent magnetization
CL	cathodoluminescence
EAO	East African Orogen
Ga	Giga annum (Latin: billion years)
IGRF90	1990 International Geomagnetic Reference Field
IMSLEK	Collection of cratons: India, northeastern Madagascar, Sri Lanka, East Antarctica, and the Kalahari craton
IRM	Isothermal Remanence Magnetization
k	kappa precision parameter
Ma	Mega annum (Latin: million years)
MIS	Malani Igneous Suite
µm	micro-meter
mT	millitesla
MSWD	mean squared weighted deviates
NRM	natural remanent magnetization
Pb-Pb	lead-lead isotope geochronology
Rb-Sr	rubidium-strontium isotope geochronology
SIMS	secondary ion mass spectrometry
TcC	Curie temperature on cooling

TcH	Curie temperature on heating
TRM	Thermal Remanent Magnetization
VGP	virtual geomagnetic pole

Abstract of Thesis Presented to the Graduate School
of the University of Florida in Partial Fulfillment of the
Requirements for the Degree of Master of Science

INDIA IN THE PROTEROZOIC: TWO KEY SPATIAL AND TEMPORAL CONSTRAINTS

By

Laura C. Gregory

May 2008

Chair: Joseph G. Meert
Major: Geology

The first paper presented in this thesis documents a paleomagnetic and geochronologic investigation undertaken on the Majhgawan kimberlite near Panna, India. 40Ar/39Ar ages on phlogopite separates from the kimberlite yield a mean age of 1073.5 ± 13.7 Ma (2s). Paleomagnetic samples from the brecciated kimberlite yielded a mean direction with a declination of 45.3° and an inclination of -25.1° (k=37, a95=9.3°). When combined with directional data from an earlier study they yield a virtual geomagnetic pole at 36.8°N, 212.5°E (dp=9.0°, dm=16.6°). This VGP overlaps with a paleomagnetic pole in the overlying Bhander-Rewa Groups (41.6° N, 32.3° E; dp=3.8°, dm=7.2°). The new age for the Majhgawan kimberlite constrains the ages of Upper Vindhyan sedimentation (Bhander-Rewa) to less than ca. 1075 Ma. The second paper within this thesis presents new paleomagnetic and geochronologic data on the Malani Igenous Suite (MIS), Rajasthan, Central India, to improve the paleogeogrpahic reconstruction of the Indian subcontinent between dispersal of the Mesoproterozoic supercontinent Rodinia and Neoproterozoic assembly of Gondwana. MIS comprises a voluminous initial phase of felsic and mafic volcanism followed by granitic plutonism. A zircon U-Pb age on a rhyolitic tuff constrains the initial volcanism in the MIS at 771 ±5 Ma. Large (up to 5 m wide) mafic dikes mark the final phase of igneous activity. A virtual geomagnetic pole

from 4 mafic dikes has a declination=358.8˚ and inclination=63.5˚ (with k=91.2 and α95=9.7). It overlaps with previously reported results from felsic MIS rocks. This normal direction includes a fine-grained mafic dikelet that showed a reversed direction with declination=195.3° and inclination=-59.7° (k=234.8 and α95=8.1°) and also records an overprint of normal polarity from the larger dikes. The VGP obtained from this study on mafic dikes is combined with previous studies of the Malani suite to obtain a mean paleomagnetic pole of 67.8˚N, 72.5˚E (A95=8.8˚). Supported by a tentative baked contact test, we argue that this pole is primary, and permits an improved reconstruction of the Indian subcontinent at around 770 Ma. Data on the MIS, and equivalent data on Seychelles at 750 ±3 Ma, are compared with paleomagnetic data on the 755 ±3 Ma Mundine Well dikes in Australia, to indicate a latitudinal separation of nearly 25° between the Indian and Australian plates. This suggest that East Gondwana was not amalgamated at ca. 750 Ma and therefore that these two cratons were assembled later into the Gondwana supercontinent, during the Pan-African ca. 550 Ma Kuunga Orogeny.

CHAPTER 1
INTRODUCTION

The Proterozoic eon quadruples the span of time represented in the Phanerozoic, yet scientific knowledge of Proterozoic geology is a small fraction compared with our understanding of the past 542 million years. A consistent problem in understanding Precambrian geology is the dearth of accurate, well-tested data. Incomplete or deformed rock records often impede accurate interpretations, and may lead instead to broad speculation for Precambrian tectonics and environments. However, well-constrained data provide crucial anchor points for generating viable scenarios that can be tested and improved. Important tools for Proterozoic geology include paleomagnetism, geochronology, detrital zircon analysis, geochemistry, stratigraphy, and structural geology- each technique with its own advantages and susceptibility to complications. Paleomagnetic data are especially useful for ancient continent reconstructions, but only when paired with precise age determinations. Paleolocations of continents provide the building blocks for understanding the dynamics of tectonic regimes, extreme environments and biological evolution during the Precambrian.

The notion of a mid- to late- Proterozoic supercontinent partially arose when similar aged paleomagnetic poles followed coinciding apparent polar wander paths (Piper, 1976; Bond et al., 1984). This supercontinent, Rodinia, amalgamated around 1.1 Ga and the subsequent breakup of major constituents was likely initiated around 750 Ma. This general concept of supercontinent assembly and breakup is oversimplified, and a more comprehensive approach reveals a complex history of plate motions associated with Rodinia constituents.

Paleolocations of the Indian subcontinent can be especially problematic. Geochronologic resolution for India in the extant literature can be greater than 500 million years for one unit, even for an intrusion that is typically emplaced within a few days (i.e. the Majhgawan kimberlite, Chapter 2). A reliable paleomagnetic pole is rendered useless when no relative age is available. The credibility of paleomagnetic data is often questioned, and every additional positive test for primary magnetization is imperitive.

A unique solution for the assembly and dispersal of supercontinent constituents can be determined only with the combination of various types of high quality, reliable data. This thesis presents two projects that add small, but significant, segments to the complex puzzle of Proterozoic tectonics. Both manuscripts included are either published or submitted to Precambrian Research.

CHAPTER 2

A PALEOMAGNETIC AND GEOCHRONOLOGIC STUDY OF THE MAJHGAWAN KIMBERLITE, INDIA: IMPLICATIONS FOR THE AGE OF THE UPPER VINDHYAN SUPERGROUP[1]

Introduction

The age of sedimentation within the Vindhyanchal basin is a controversy that has been disputed for over one hundred years (Venkatachala, 1996). While the age of the Lower Vindhyan Group is now well constrained, the Upper Vindhyan section has yet to be dated with any certainty. The onset of sedimentation in the Vindhyanchal basin commenced sometime after 1850 Ma based on U-Pb ages from underlying volcanic rocks (Deb et al., 2002). Geochronologic data from the Lower Vindhyan sequence (Figure 2-1a; Table 2-1) are derived from U-Pb ages on porcellanites that yield 1628 ±8 Ma, 1631.2 ± 5.4 Ma and 1630.7 ± 0.8 Ma (Rasmussen et al., 2002; Ray et al., 2002). Ages from the Rampur ash beds, below the Rhotas limestone, yield SHRIMP Pb-Pb ages of 1592 ± 12 Ma and 1602 ± 10 Ma. Less precise Pb-Pb from carbonate yielded ages of 1599 ± 48 Ma (Sarangi et al., 2004) and 1601 ± 130 Ma (Ray et al., 2003) for the Rhotas limestone.

In comparison, the Upper Vindhyan sedimentary rocks lack reliable age constraints. Ray et al. (2003) reported a very poorly defined Pb-Pb age on the Bhander Limestone of 750 Ma that they considered unreliable. Ray et al. (2003) also used Sr-isotopic data on the limestones to estimate a ca. 750 or 650 Ma age for the Bhander limestones; however, the Sr-isotopic data are also consistent with older and younger sections of the global curve. De (2003) reported ‘Ediacaran-like’ organisms with very poor preservational characteristics from the Bhander limestone that are consistent with the estimate by McElhinny et al. (1978) of an Ediacaran-

[1] Reprinted with permission from Gregory, L.C., Meert, J.G., Pradhan, V.R., Pandit, M.K., Tamrat, E., Malone, S.J., 2006. A paleomagnetic and geochronologic study of the Majhgawan kimberlite, India: Implications for the age of the Upper Vindhyan Supergroup. Precambrian Research 149, 65-75.

Cambrian age for the Bhander-Rewa Groups. McElhinny et al. (1978) compared directions in the Bhander-Rewa rocks to known Cambrian rocks from the Salt range in Pakistan. A more recent paper by De (2006) yields Ediacaran fossils with much better preservation in the Lhakeri Limestone (Bhander Group). If the fossil find is confirmed by future work, then the Bhander Group is Ediacaran aged (ca. 635-542 Ma; Condon et al., 2005; Jiang et al., 2003; Zhang et al., 2005).

The Majhgawan Kimberlite, that intrudes Upper Vindhyan rocks (Figure 2-1b,c), is important for obtaining a more reliable age for the basin due to its stratigraphic location (intruding the Kaimur sandstones). The reported age of Majhgawan from previous studies range from 1630 ± 353 Ma to 947 ± 30 (see Table 1; also Auden, 1933). The kimberlite was dated by Crawford and Compston (1970) with mica to yield an age of 1116 ± 12 Ma. Two K-Ar whole rock and one mica determination yielded ages of 947 ± 30, 1170 ± 46 (whole rock, Paul et al., 1975) and 1056 (mica, Crawford and Compston, 1970). Two recent ages of 1044 ± 22 Ma and 1067 ± 31 Ma were reported using Rb-Sr (Smith, 1992; Kumar and Gopalan, 1992 respectively). The Majhgawan Kimberlite is located in Madhya Pradesh, India (Figure 2-1). It is one of several Proterozoic-age kimberlites/lamproites intruding the peninsular Indian crust. Other major bodies thought to be broadly consanguineous with the Majhgawan kimberlites are the Lattavaram, Wajrakur, Narayanpet and Mulligiripalle kimberlites of the Dharwar craton (Miller and Hargaves, 1994; Haggerty and Birkett, 2004) and the Hinota pipe (Aravalli craton). Not all of these kimberlites have reliable age constraints. The Wajrakur kimberlite has ages ranging from 840-1350 Ma (Paul, 1979; Crawford and Compston, 1973; Paul et al., 1975). The Lattavaram kimberlite is dated between 933-1505 Ma (Paul, 1979; Paul et al., 1975). A U-Pb (perosvkite) age of 1079 was cited in Miller and Hargraves (1994) for the Muligiripalle kimberlite. The

Lattavaram, Wajrakur and Mulligiripalle pipes have also been studied paleomagnetically by Miller and Hargraves (1994). The Wajrakur samples were unstable and yielded no useful data whereas the Lattavaram and Mulligiripalle pipes yielded similar paleomagnetic data, although the site statistics showed poor grouping and large errors. Miller and Hargraves (1994) conducted a paleomagnetic study of Majhgawan and reported a paleomagnetic pole at 38.9˚ N, 216.5˚ E.

Geology of the Kimberlite

The Majhgawan kimberlite intrudes Baghain sandstone in the upper Kaimur Group, which lies below the Bhander-Rewa sequence in the Upper Vindhyan basin (Figure 2-1). The body is pear shaped with steeply dipping walls (80°) and its surface originally outcropped over an area of 500 x 320 m (Chatterjee and Rao, 1995). Deformation of the Baghain sandstone is severe in the vicinity of the pipe. The Kaimur rocks have been shattered and tilted inward toward the pipe, but elsewhere in the region the Baghain sandstone and overlying rocks of the Bhander-Rewa Groups have very low dips (< 10°) or are undeformed. The pipe has a variable lithology and is composed of concentrically arranged units. The classification of the pipe is debated as it has characteristics of both a kimberlitic intrusion and an olivine lamporitic tuff. Chatterjee and Rao (1995) classify it as an intermediate between the two. The kimberlite is observed to have three intervals of intrusion: (1) deep-green brecciated kimberlite; (2) botryoidal zone of kimberlite contaminated by shale xenoliths; and (3) basaltic kimberlite. The pipe is mined for diamonds and also contains megacrysts of olivine, phlogopite, ilmenite, pyrope and enstatite with phologopite mica as a constituent of a serpentine and calcite matrix (Mukherjee et al., 1997). Phlogopite megacrysts can be placed into two distinct groups. Megacrysts are either rounded and commonly weathered or hexagonal and fresh (Mukherjee et al., 1997).

Intraformational conglomerates within the Rewa Group near Panna are diamond-bearing suggesting that the deposition of the Rewa Group post-dates intrusion of the kimberlite (Mathur, 1962, 1981). Rau and Soni (2003) examined the provenance of the diamondiferous conglomerates in the Rewa Group and concluded that the source for the diamonds in the Rewa Group may be something other than the nearby Majhgawan or Hinota pipes. No significant erosional surfaces are present in between the Kaimur, Rewa and Bhander Groups.

Paleomagnetism

Paleomagnetic Experiments

Samples were drilled in the field using a gasoline powered drill and oriented using magnetic and sun compasses. Sun compass readings were used to correct for the local declination and any rock magnetic interference. Limited outcrop and security concerns allowed us to collect only 10 samples from two sites in the brecciated kimberlites and basaltic kimberlites. Samples were cut into standard specimens and stored in a magnetically shielded room at the University of Florida paleomagnetic laboratory. Preliminary samples were stepwise treated using thermal or alternating field demagnetization and after evaluation, a series of demagnetization steps was chosen. Alternating field demagnetization was conducted using a home-built AF-demagnetizer and with fields up to 100 mT. Thermal demagnetization was conducted up to temperatures of 600˚C with an ASC-Scientific thermal demagnetizer and all samples were measured in a ScT Cryogenic magnetometer. Principle component analysis (Kirschvink, 1980) was used to determine the best fit lines for each sample.

Rock Magnetic Experiments

The susceptibility of each sample was measured before treatment on an Agico SI-3B bridge. In order to further characterize magnetic carriers, Curie temperature runs were conducted on several powdered samples using a KLY-3S susceptibility bridge adapted with a CS-3 heating unit. For this experiment, susceptibility is measured incrementally during heating and cooling of the samples. Isothermal remanence acquisition studies (IRM) were also conducted on select samples.

Geochronology

Samples of micaceous brecciated kimberlite were crushed, sieved and phlogopite separates were hand picked. The individual phlogopite samples were then ultrasonically cleaned and rinsed several times. The grains were examined again under microscope and any grains with weathered margins or impurities were discarded. The grains were then wrapped in aluminum foil and sent to Oregon State University's irradiation facility. Gas from the samples was stepwise treated using CO2 irradiation laser and measured on a MAP215-50 mass spectrometer. The flux monitor was GA1550 biotite (age 98.8 ± .5 Ma; Renne et al., 1998) and analyses were performed by James Vogl.

Results

Geochronology

The phlogopite micas contain roughly 10% K2O (Mukherjee et al., 1997). Standard mineral separation and 40Ar/39Ar techniques were followed (see methods) on two splits of large grains of unweathered phlogopites. Results for stepwise degassing of the samples are shown in Figure 2-2a (analytical results are given in Table 2-3, errors reported are 2s). The first split yields a well-defined plateau at 1061.7 ± 9.7 Ma (66% of the gas, MSWD= 1.02) and a total fusion age of 1068.2 ± 9.4 Ma. The isochron age for split #1 is 1068.3 ± 14.0 Ma with a low MSWD of 0.46 (Figure 2-2b). The second split yields a concordant plateau age of 1078.4 ± 11.4 Ma (82% of the gas, MSWD=3.31) and a total fusion age of 1080 ± 10 Ma (Figure 2-2c). The isochron age for split #2 is 1072.2 ± 21 Ma with an MSWD of 2.70. Our best estimate for the age of the phlogopite micas from Majhgawan is given by a weighted mean of the ages within the plateau segments of both samples, which is 1073.5 ± 13.7 Ma.

Kimberlites and lamproites are both thought to be emplaced into the shallow crust on time scales ranging from several hours to several days (Skinner and Marsh, 2004). Thus, the age of the phlogopites should closely date the time of upper crustal emplacement and also the age of the magnetization in the rocks.

Paleomagnetism

A total of 10 samples were collected from the brecciated kimberlite and basaltic kimberlite (eight samples exhibited stable demagnetization behavior). Typical demagnetization behavior is shown in Figure 2-3 using both alternating field (Figure 2-3a) and thermal (Figure 2-3b) treatments. Alternating field treatments up to 60 mT removed over 90% of the natural remanent magnetization (NRM). Thermal demagnetization was applied up to temperatures of 600°C and a loss of 90% of initial NRM strength occurred at about 550°C with a discrete unblocking temperature range between 500 and 550°C. The mean direction from our samples is D=45.1°, I=-25.1° (k=37 and a95=9.3°; Figure 2-4)

Paleomagnetic data from Majhgawan, including the data from Miller and Hargraves (1994) yield a mean direction with a declination of 37.5° and an inclination of -26.5° (k=66 and a95=15.3°; Figure 2-4) with a virtual geomagnetic pole (VGP) of 36.8°N, 212.5°E (dp=9.0, dm=16.6; Figure 2-4). The VGP translates to a site latitude of 14° +/-8.3°/10°. Rock magnetic and demagnetization behavior (Figures 2-3 and 2-5) indicate the primary carrier is magnetite. Curie temperature runs (Figure 2-5) show a sharp drop in susceptibility at 591.3°C and 605.1°C, which are both slightly above the Curie temperature for magnetite. Isothermal remanence magnetization tests show a rapid rise in intensity and near saturation at 0.4 to 0.7 Telsa. The rock magnetic tests and demagnetization behavior are both characteristic of magnetite with perhaps a small contribution from hematite. Petrographic observations were described in Miller and Hargraves (1994) who noted the presence of fine magnetite grains in the matrix and within mica flakes which in some cases had been altered to hematite. These observations are consistent with the rock magnetic data collected during our study (Table 2).

Discussion and the Age of the Upper Vindhyan

The age of the Upper Vindhyan sequence is contentious. Previous estimates on the age of Kaimur-Rewa and Bhander Groups unrealistically span over 1 billion years, from 1650 Ma to as young as Ordovician (Ray, 2006; Auden, 1933). The Bhander-Rewa Groups are at the center of this argument because they are generally considered to be Neoproterozoic in age (750-650 Ma; Ray et al., 2003; Kumar et al., 2002). The age estimates of Ray et al. (2003) and Kumar et al. (2002) are based primarily on the comparison to global curves of 87Sr/86Sr ratios and d13C dates from the Bhander and Lhakeri limestones. These ratios were used to argue for an age of Bhander sedimentation between 750 and 650 Ma. A 750 Ma age for the Bhander limestones is precluded by the assumption of a primary magnetization carried in the Bhander-Rewa rocks (McElhinny et al., 1978). India has a well-defined paleomagnetic pole at 750 Ma derived from the Malani Igneous Suite (Torsvik et al., 2001) that is distinct from the published Bhander-Rewa directions (Figure 2-3). A late Neoproterozoic or Cambrian age for the Bhander-Rewa was supported by a comparison between paleomagnetic directions from Late Proterozoic-Cambrian age sedimentary rocks in the Salt Ranges of Pakistan (Ref, McElhinny et al., 1978; Meert, 2003). Although the paleomagnetic poles from the Salt Range rocks are similar to the Bhander-Rewa directions, Klootwijk et al. (1986) demonstrated significant vertical axis rotation of units in the Salt Ranges (up to 45˚) during the Tertiary negating the validity of comparisons between these units.

Additional evidence forwarded in support of a Neoproterozoic age is generally poor. The previously noted fossils from De (2003) do not provide a well-constrained date. Identification of the impressions as Ediacaran is problematic; however, more recently documented fossils (De, 2006) from the same region show much better preservational characteristics and would suggest that the Lhakeri limestone is younger than ca. 635 Ma. Chakrabarti (1990) also documents possible trace fossils in the Bhander Group. These are noted as burrow zones with large diameter burrows (0.5-4.5 cm) and micro-burrows (less than 1.5 mm) that are lined with a thin layer of clay. Yet it is mentioned that these traces may be dubiofossils produced by either sand collapse or fluid escape. Nevertheless, Chakrabarti (1990) suggested a Riphean age (1400-800 Ma) for the Bhander-Rewa Groups. Both Chuaria and Tawuia fossils have been found in the Bhander-Rewa (Rai et al., 1997; Kumar and Srivastava, 2003), but the age range of Chuaria may span as far back as the Paleoproterozoic (Steiner, 1997) and thus they are not useful as index fossils for the Neoproterozoic. Chuaria and Tawuia are reported in the Suket shales of the Lower Vindhyan Semri Group (Kumar, 2001). Steiner (1997) gives a preferred range for the Chuaria-Tawuia assemblage from 1000-700 Ma.

Lastly, although the exact number of glaciations and the extent of those glaciations are debated, the Neoproterozoic is known for the presence of glaciogenic sequences on nearly all the continents (Evans, 2002). The Upper Vindhyan sequence shows only cryptic evidence of glaciogenic sediments despite a nearly continuous record of sedimentation (Prasad, 1984; Kumar et al., 2002). Kumar et al. (2002) noticed a large negative shift in $\delta^{13}C$ values in the Lhakeri limestone (Bhander Group, Rajasthan) and argued that it might represent a peninsular India equivalent of a cap-carbonate. Kumar et al. (2002) also mentioned the occurrence of 'tilloid' rocks beneath the Lhakeri limestone in Rajasthan as potential representatives of the 'Snowball Earth' glaciation. In contrast, the Lhakeri limestone in the Son Valley section shows no negative d13C excursion (Ray et al., 2003) suggesting either that (a) previous correlations of these units is incorrect or (b) one of the carbon studies is incorrect or (c) carbon isotopic rations show lateral variations across the basin (see also Kaufman et al., 2006). Our geochronologic data from the

Majhgawan kimberlite suggests that the Bhander-Rewa Groups are both younger than ca. 1075 Ma.

Paleomagnetic data from our study along with previous studies of the Majhgawan kimberlite (Miller and Hargraves, 1994) and the Bhander-Rewa Groups (McElhinny et al., 1978) present an intriguing alternative interpretation for the age of the Upper Vindhyan. Prior paleomagnetic studies have been reported on the Bhander-Rewa Groups overlying the Majhgawan kimberlite (McElhinny et al., 1978, Klootwijk et al., 1973; Athavale, 1963). The paleomagnetic directions from the Bhander-Rewa yield a mean declination of 34.2° and an inclination of -20.3° (k=35, a95=7°). This compares favorably with the Majhgawan data reported in this study and that by Miller and Hargraves (1994; Figure 2-3).

There are several explanations for the similarity in directional data from the Majhgawan kimberlite and the Bhander-Rewa Groups. One option is that they are both remagnetizations of Neoproterozoic or Cambrian age. Other possibilities are (a) that the Mesoproterozoic directions in the Majhgawan kimberlite are fortuitously identical to the much younger Bhander-Rewa Group (b) the kimberlite was remagnetized during Bhander-Rewa time or (c) unrecognized tilting of the Majhgawan kimberlite might result in the incorrect use of the in-situ directions. A final possibility is that the Bhander-Rewa Groups are only slightly younger than the Majhgawan kimberlite. At present, we feel comfortable rejecting the possibility of unrecognized tilting of the kimberlite. Tilting of the Kaimur sandstone away from the intrusion is minor (<10˚) and therefore any post-intrusion tilting is likely to be minor as well. The other explanations require a detailed paleomagnetic study of the Bhander and Rewa Groups. We are currently in the process of completing such a study.

Conclusions

Our geochronologic study of Majhgawan yields a well constrained 40Ar/39Ar age of 1073.5 ± 13.7 Ma and a virtual geomagnetic pole at 36.8°N, 212.5°E (dp=9.0, dm=16.6) that is similar to previously published paleomagnetic poles in the overlying Bhander-Rewa Groups (41.6° N, 212.3° E; dp=3.8°, dm=7.2°). Our age helps constrain the age of sedimentation in the Upper Vindhyan Bhander and Rewa Groups to less than 1075 Ma.

Acknowledgements: The authors would like to acknowledge support from the National Science Foundation EAR04-09101 (to JGM), Jim Vogl for his assistance in acquiring and analyzing the argon data in this paper, for Linda Sohl, Dhiraj Banerjee and Bob Tucker for their assistance in the field.

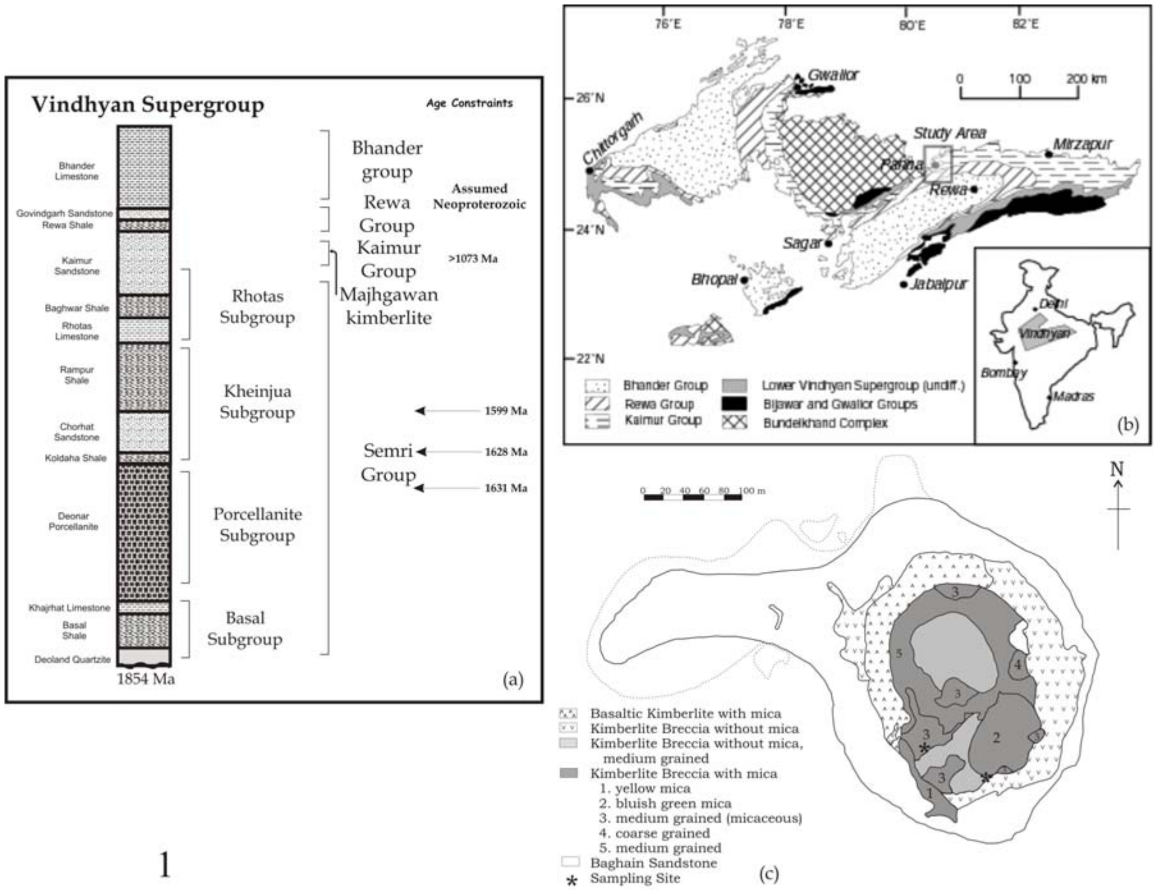

Figure 2-1. Generalized stratigraphic column, regional and local geologic map. (a) Generalized stratigraphic column of the Vindhyan Supergroup shown with radiometric age constraints. The Majhgawan kimberlite intrudes the Kaimur sandstone of the Upper Vindhyan. (b) Geologic map of the region including the Vindhyanchal basin and the study area near Panna, India. (c) geologic map of the Majhgawan kimberlite (after Chatterjee and Rao, 1995). Sampling locations for paleomagnetism were taken from the basaltic kimberlite and the brecciated kimberlite. Samples from the Miller and Hargraves (1994) study were solely from the brecciated kimberlite.

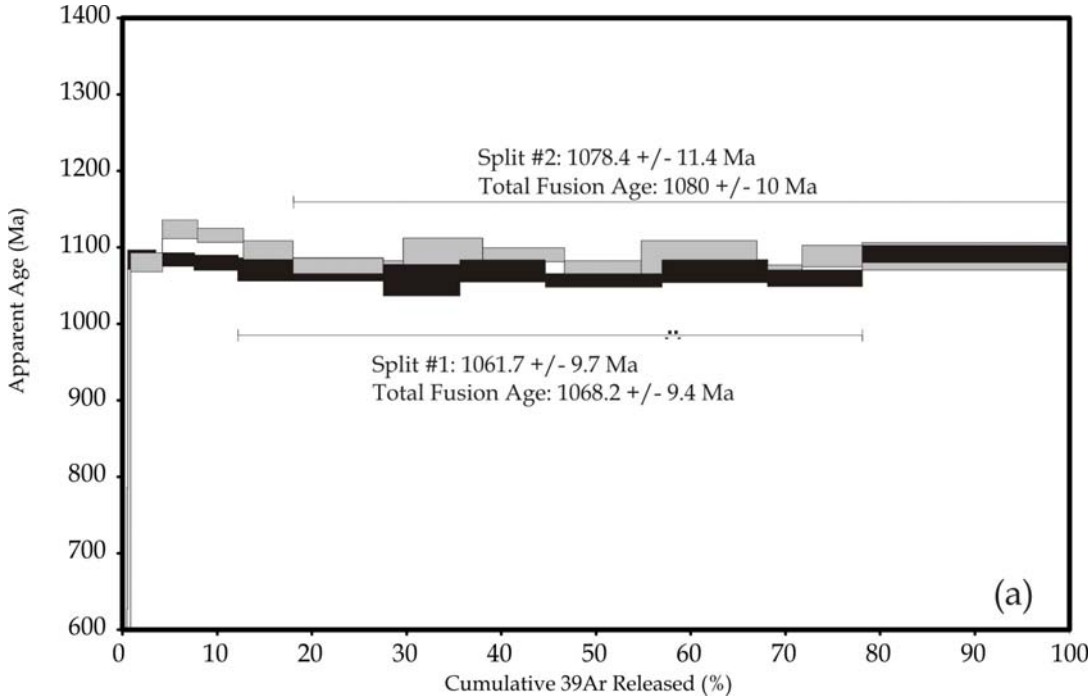

Figure 2-2. Stepwise degassing spectrum for Majhgawan phlogopites (2 splits). Both show well-defined plateaus that overlap at the 2s level. The average age obtained from a weighted mean of plateau steps for splits 1 and 2 is 1073.5 ± 13.7 Ma

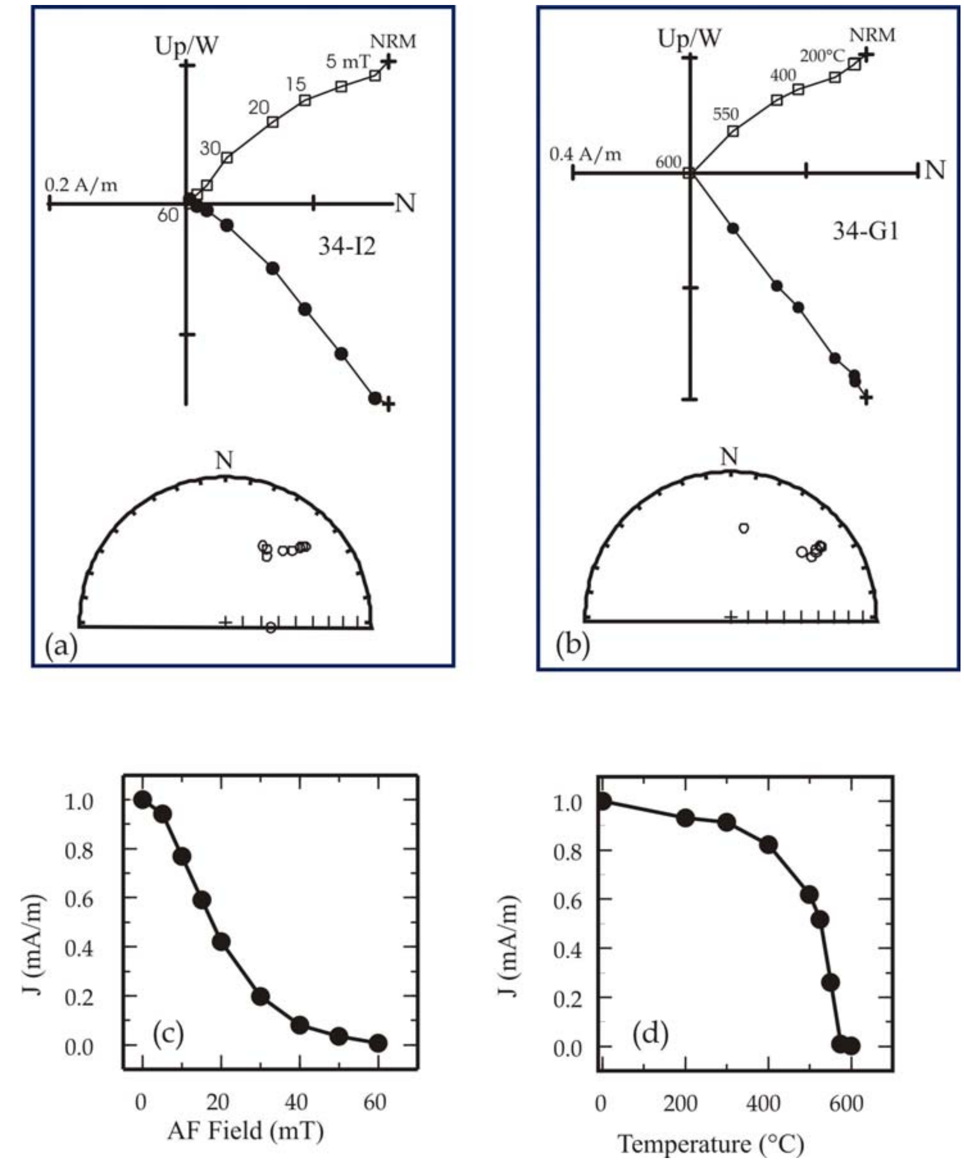

Figure 2-3. Zijderveld plots, stereoplots, and thermal/AF demagnetization trends for select samples. (a) Thermal demagnetization Zijderveld plots for a brecciated kimberlite sample showing univectorial behavior (b) Alternating field demagnetization Zijderveld plot for a brecciated kimberlite sample showing univectorial behavior. (c) Intensity decay plot for thermally demagnetized sample and (d) Intensity decay plot for an alternating field demagnetized sample.

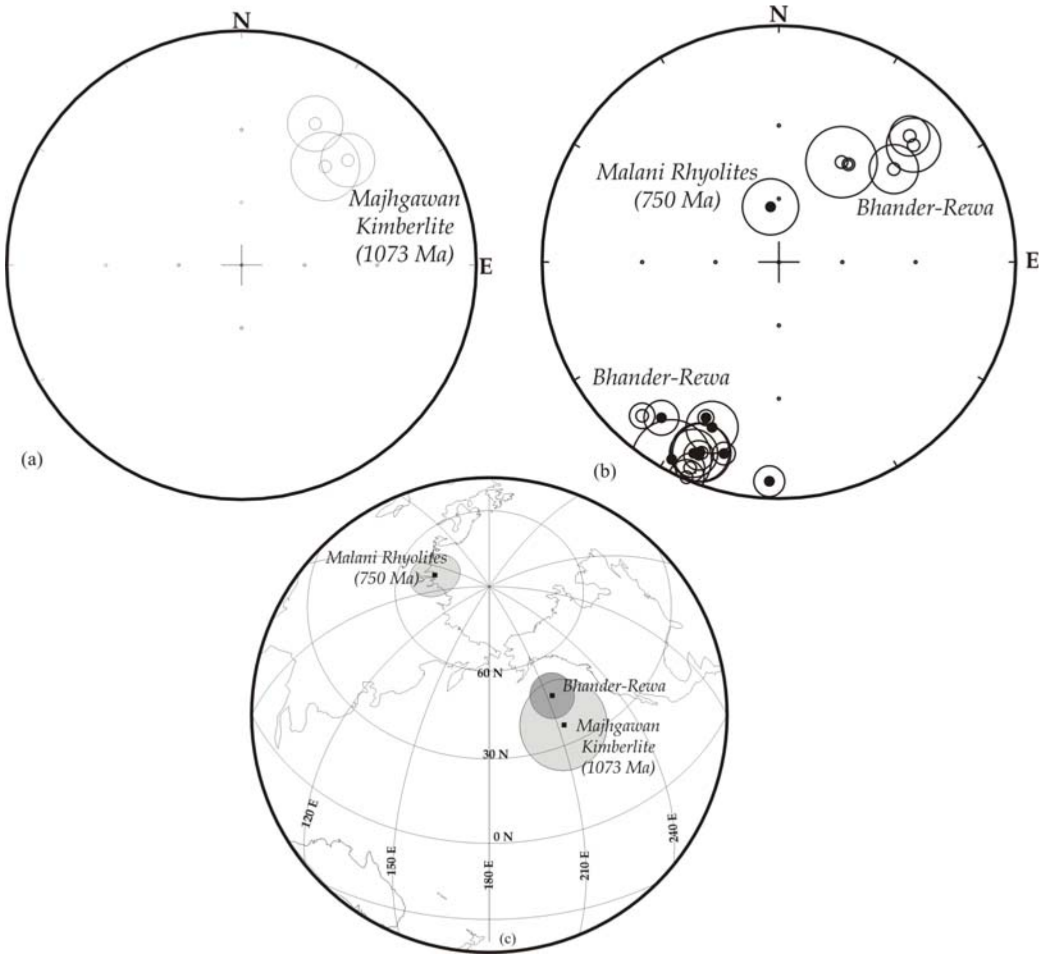

Figure 2-4. Site mean directions, paleomagnetic and virtual geomagnetic poles for critical rock units. (a) Site mean directions (tilt-corrected) from 14 sites in the Bhander and Rewa Groups obtained in an ongoing study by the authors (reported in Malone et al., 2005) and are identical to those reported previously by McElhinny et al., 1978 for the Bhander and Rewa Groups (b) Site means for three sites in the Majhgawan kimberlite collected in this study and also the results of Miller and Hargraves (1994). We also show the combined mean pole for the Malani igneous province including results from late-stage Malani dykes reported in Gregory et al. (2005). (c) Paleomagnetic and virtual geomagnetic poles for the Bhander-Rewa Groups, the Malani Igneous province and the Majhgawan kimberlites.

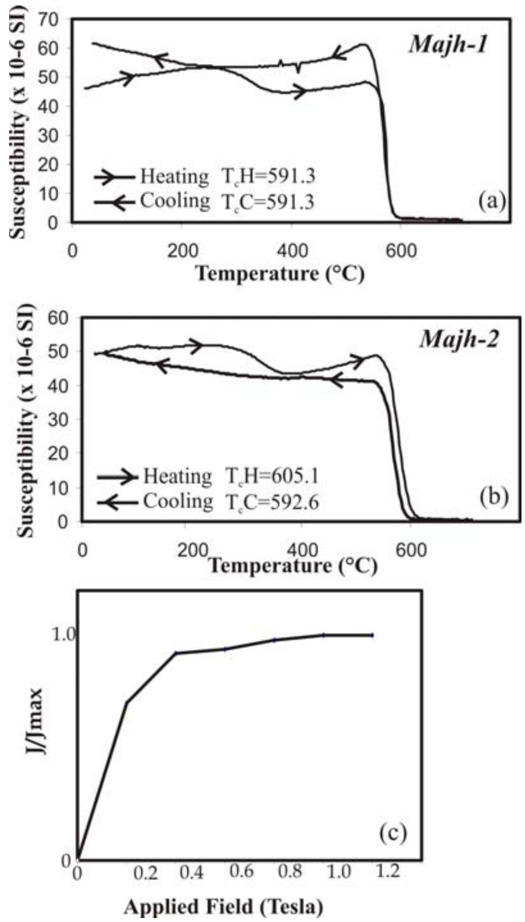

Figure 2-5. Magnetic characterization data. (a) Temperature-Susceptibility graph for a sample of the Majhgawan kimberlite showing a heating and cooling Curie temperature of 591.3° C. (b) Temperature-Susceptibility graph for a sample of the Majhgawan kimberlite showing a heating Curie temperature of 605.1° C and a cooling Curie temperature of 592.6° C. (c) Isothermal remanence acquisition curve for a sample of Majhgawan kimberlite showing saturation at 0.4 Tesla.

Table 2-1. Age constraints on Vindhyan sedimentary sequences.

Stratigraphic Layer	Method	Age Ma	Reference
Upper Vindhyan:			
Bhavpura Shale (Bhander)	K-Ar	550	Crawford and Compston 1970
Bhander Limestone	Pb-Pb	650	Ray et al., 2003
Bhander Limestone	Sr-isotopes	750	Ray et al., 2003
Bhander Limestone	fossils	Ediacaran-Cambrian	De, 2003
Kaimur Conglomerate	K-Ar	940	Vinogradov et al., 1964
Kaimur Conglomerate	K-Ar	1071.6 ± 169.3	Srivastava and Rajagopalan, 1988
	F-T	1070.5 ± 160.4	Srivastava and Rajagopalan, 1988
Lower Vindhyan:			
Rotasgarh Limestone	K-Ar	1400 ± 70	Vinogradov et al., 1964
Rotasgarh Limestone	Pb-Pb	1601 ± 130	Ray et al., 2003
Rohtas formation	Pb-Pb	1599±48	Sarangi et al., 2004
Rampur formation	K-Ar	1110 ± 60	Vinogradov et al., 1964
Rampur formation	K-Ar	1124.5 ± 157.8	Srivastava and Rajagopalan, 1988
Rampur ash beds	Pb-Pb	1592 ± 12	
		1602 ± 10	
Porcellanites	U-Pb	1628 ±8	Rasmussen et al., 2002
		1631.2 ± 5.4	Rasmussen et al., 2002
		1630.7 ± 0.8	Ray et al., 2002
Kimberlites:			
Majhgawan Kimberlite	**Ar-Ar**	**1073± 13.7**	**This study**
Majhgawan Kimberlite	K-Ar	1116± 12	Crawford and Compston, 1970
Majhgawan Kimberlite	K-Ar	947± 30	Paul et al., 1975
Majhgawan Kimberlite	K-Ar	1170±46	Paul et al., 1975
Majhgawan Kimberlite	K-Ar	1056	Crawford and Compston, 1970
Majhgawan Kimberlite	Rb-Sr	1044±22	Smith, 1992
Majhgawan Kimberlite	Rb-Sr	1067±31	Kumar et al., 1993
Wajrajur kimberlite	Rb-Sr	1350±294	Paul, 1979
Wajrajur kimberlite	Rb-Sr	1116	Crawford and Compston, 1973
Lattavaram kimberlite	Rb-Sr	1505	Paul, 1979
Lattavaram kimberlite	K-Ar	933	Paul et al., 1975
Muligiripalle kimberlite	U-Pb	1079	Miller and Hargraves, 1994

Table 2-2. Summary of paleomagnetic results.

Study	Ns(#samples)	Dec	Inc	K	α_{95}	Pole Lat	Pole Long	dp	dm
Majhgawan									
This paper	8	45.3°	25.1°	37	9.3	33.5°N	203.3°E		
Miller and Hargraves site 1[1]	6	40.2	-32.3	28	12.8	32.4° N	213.2° E		
Miller and Hargraves site 2[1]	6	27.4	-21.6	54	9.2	45.3° N	220.1° E		
Mean of 3 sites	*22*	*37.5°*	*26.5°*	*66*	*15.3*	*36.8°N*	*212.5°E*	*9.0°*	*16.6°*
Malani Mean[2]	4 Studies	359.1°	62°	73.17	7.9	72.7° N	70.5° E	9.5	12.3
Bhander-Rewa Mean[3]	18 Sites	34.2°	20.3°	21.2	7	41.6°N	212.3°E	3.8°	7.2°

Ns= number of sites or #samples; Dec=declination; Inc=inclination; α95= circle of 95% confidence; Pole lat=latitude of the paleomagnetic pole; Pole long=longitude of paleomagnetic pole; (dp,dm) cone of 95% confidence about the paleomagnetic pole in the co-latitude direction (dp) and at a right angle to the co-latitude direction (dm), [1] Miller and Hargraves (1994), [2] Mean reported from Klootwijk et al (1975), Athavale et al. (1963), Torsvik et al. (2001) and Gregory et al. (2005), [3] Mean reported from McElhinny et al. (1978).

Table 2-3. Analytical Data

Power (watts)	36Ar Volts	37Ar Volts	39Ar Volts	40Ar Volts	40Ar* %	40Ar*/39Ar	Cumulative 39Ar (%)	Calculated age (Ma)	Error in age (± 2 s.d.)	K/Ca
Majh01 biotite; J = .00384										
0.11 (2.1)	0.00067	0.00024	0.00126	0	0	0.00000	0.11	0	± 0.00	2.26
0.21(2.3%)	0.00013	0.00061	0.00134	0.03697	49.84	27.68094	0.12	182.24	± 109.22	0.949
0.32 (2.6%)	0.001	0.00792	0.00224	0	0	0.00000	0.2	0	± 0.00	0.122
0.42 (3%)	0.00012	0.00147	0.00153	0.19068	84.56	124.67805	0.14	705.77	± 79.65	0.448
0.74 (3.8%)	0.00026	0.00218	0.03306	7.07956	98.91	214.17018	2.94	1082.74	± 12.57	6.526
0.80 (5%)	0.00004	0.00018	0.04522	9.68697	99.87	214.23648	4.02	1082.99	± 8.40	110.226
0.85 (4.0%)	0.00006	0.00036	0.05248	11.18651	99.82	213.15344	4.66	1078.87	± 9.84	62.358
0.95 (4.2%)	0.00022	0.00294	0.17232	36.33149	99.81	210.83660	15.32	1070.02	± 14.83	25.176
1.0 (4.4%)	0.00013	0.0018	0.09053	18.76306	99.79	207.25576	8.05	1056.26	± 20.53	21.625
1.06 (4.6%)	0	0.00382	0.10145	21.34383	99.99	210.38313	9.02	1068.28	± 14.41	11.425
1.16 (4.9%)	0.00036	0.00368	0.13838	28.65372	99.61	207.05847	12.3	1055.5	± 8.87	16.163
1.27 (5.2%)	0.00002	0.00088	0.12529	26.35047	99.97	210.30834	11.14	1068	± 14.83	61.311
1.38 (5.4%)	0.00003	0.00114	0.11219	23.37715	99.95	208.38027	9.97	1060.59	± 12.97	42.283
fused	0	0.00019	0.24779	53.66914	99.99	216.59434	22.02	1091.93	± 12.90	563.464
Majh2 biotite; J = 0.00384										
0.42 (3.1%)	0.00240	0.00161	0.00655	0.05114	6.72	7.80610	0.84	53.28	± 62.08	1.748
0.74 (3.8%)	0.00120	0.00000	0.02612	5.57510	94.03	213.44767	3.36	1079.99	± 11.96	0.000
0.85 (4.1%)	0.00081	0.00000	0.02899	6.52504	96.44	225.05125	3.73	1123.63	± 11.78	0.000
0.95 (4.3%)	0.00046	0.00000	0.03769	8.40122	98.40	222.90544	4.85	1115.64	± 9.06	0.000
1.06 (4.5%)	0.00030	0.00000	0.04095	8.91638	99.01	217.75048	5.27	1096.30	± 12.24	0.000
1.16 (4.7%)	0.00077	0.00334	0.09027	19.11802	98.81	211.79462	11.61	1073.69	± 8.44	11.637
1.16 (4.8%)	0.00113	0.00139	0.06515	14.16368	97.68	217.38796	8.38	1094.93	± 16.83	20.122
1.16 (4.9%)	0.00054	0.00287	0.06728	14.54292	98.90	216.14813	8.65	1090.24	± 9.15	10.094
1.16 (5.1%)	0.00047	0.00300	0.06300	13.28969	98.96	210.96016	8.10	1070.49	± 11.77	9.016
1.38 (5.4%)	0.00033	0.00186	0.09505	20.39615	99.51	214.57669	12.22	1084.28	± 24.72	21.950
1.48 (5.6%)	0.00015	0.00000	0.03697	7.76653	99.40	210.09280	4.75	1067.17	± 10.00	0.139
fused	0.00184	0.00134	0.21955	47.23523	98.85	215.15006	28.23	1086.46	± 16.11	70.453

(1) Atmospheric argon, (2) Calcium interference, (3) Radiogenic argon, (4) Percent of argon gas released, (5) J parameter is the standard flux monitor used to normalize the amount of K converted to Ar during irradiation

CHAPTER 3
PALEOMAGNETISM AND GEOCHRONOLOGY OF THE MALANI IGNEOUS SUITE, NORTHWEST INDIA: IMPLICATIONS FOR THE CONFIGURATION OF RODINIA AND THE ASSEMBLY OF GONDWANA[2]

Introduction

The notion of a Meso- to Neoproterozoic supercontinent formed in the aftermath of Grenvillian orogenesis began to develop in the 1970's (Piper, 1976; Bond et al., 1984). The name of 'Rodinia' was proposed in the early 1990's (McMenamin and McMenamin, 1990; Dalziel, 1991; Moores, 1991; Hoffman, 1991). There are myriad configurations proposed for the Rodinia supercontinent and the exact paleolocations of its constituents are unresolved (Dalziel, 1991; Moores, 1991; Hoffman, 1991, Meert and Torsvik, 2003; Li et al., 2008). The archetypal model for Rodinia outlines that the supercontinent began to form at about 1300 Ma and reached maximum size at about 1000 Ma. Fragmentation and breakup of Rodinia was initiated sometime between 800-700 Ma along a rift between western (present-day coordinates) Laurentia and East Antarctica-Australia (Bond et al., 1984; Dalziel 1991; Hoffman, 1991; Powell et al., 1993). It is hypothesized that this rifting heralded a period of intense global cooling, sparking the development of multi-cellular life on Earth (Hoffman, 1998;Meert and Lieberman, 2008). Knowledge of the distribution and geotectonic evolution of continents related to Rodinia breakup is critical for an improved understanding of the context and causes of extreme climatic changes and accelerated biologic evolution at the enigmatic boundary between the Neoproterozoic and the Paleozoic.

The assembly of the supercontinent Gondwana followed the fragmentation of Rodinia. Eastern Gondwana comprised cratonic blocks that are currently within India, Madagascar, Sri

[2] Reprinted with permission from Gregory, L.C., Meert, J.G., Bingen, B., Pandit, M.K., Torsvik, T.H., 2008. Paleomagnetism and Geochronology of the Malani Igneous Suite, Northwest India: Implications for the configuration of Rodinia and the assembly of Gondwana. Precambrian Research, submitted.

Lanka, East Antarctica, Australia and the Seychelles. The paleogeography of these cratons prior to the formation and after breakup of Rodinia is not well constrained. Some (Windley et al., 1994; Piper, 2000; Yoshida and Upreti, 2006; Squire et al., 2006; Paulsen et al., 2007) argue that these cratons came together in a single collisional event around or even earlier than 1300 Ma, were fused in that same configuration within Rodinia, and remained so until the breakup of Gondwana in the Mesozoic. More consistent with available geologic, paleomagnetic and geochronologic data is the alternative formation of eastern Gondwana as a polyphase assembly of cratonic nuclei that were severed and separately dispersed from the Rodinia supercontinent (Meert et al., 1995; Meert and Torsvik, 2003; Meert, 2003; Boger et al., 2002; Fitzsimons, 2000; Pisarevsky et al., 2003; Collins and Pisarevsky, 2005). This dispute may ultimately be resolved through the acquisition of high-quality paleomagnetic data coupled to high-resolution geochronologic ages from the various cratons that comprise Gondwana. Unfortunately, many extant studies are incomplete in that they do not incorporate an age with paleoposition and thus do not place strong spatial-temporal constraints on ancient continent localities.

The location of India within Gondwana is critical for evaluating the various tectonic models related both to the assembly of greater Gondwana and models of Rodinia. Greater India is placed alongside East Antarctica in the traditional Gondwana fit at 560 Ma (Figure 3-1; deWit et al., 1988), and some extrapolate the India-Antarctica-Australia connection to exist within Rodinia and even earlier supercontinents (Dalziel, 1991; Li et al., 1996; Weil et al., 1998; Owada et al., 2003). However, due to paleomagnetic and geologic correlations (or lack thereof), many workers have since suggested that India maintained a significant latitudinal offset from the archetypal Gondwana fit with Antarctica (Fitzsimons, 2000; Torsvik et al., 2001a; Powell and Pisarevsky, 2002).

The Malani Igneous Suite (MIS) in northwest India provides potentially critical paleomagnetic and geochronologic data for the Indian subcontinent during the late Neoproterozoic. Outcropping near Rajasthan (Figure 3-2), the MIS is estimated to be one of the largest felsic igneous suites in the world (51,000 km2; Pareek, 1981; Bhushan, 2000). Paleomagnetic studies from the MIS are thought to define the key paleomagnetic pole for the Indian subcontinent at ca. 750 Ma. In this study, we augment previous work via the addition of paleomagnetic data from late-stage mafic dikes along with precise U-Pb ages from the earlier erupted rhyolitic tuffs. Combined, these data contribute a key paleopole for the Indian plate during the Neoproterozoic, and lead to a discussion on the drift of India between the diffusion of Rodinia and the formation of Gondwana

Geology and Tectonic Setting

Magmatism in the MIS occurred in three phases. Activity commenced with an initial volcanic phase made up of basaltic then felsic flows. The second phase is characterized by the intrusion of granitic plutons. Predominately felsic and minor mafic dike swarms form the third and final phase of the igneous cycle. Malani felsic rocks are un-metamorphosed, but slightly tilted and folded. Late stage mafic dikes are all vertical to sub-vertical (Figure 3-3). The MIS unconformably overlies Paleo- to Mesoproterozoic metasediments, and basement granite gneisses and granodiorites of an unknown age (Pandit et al., 1999). The suite is unconformably overlain by the flat-lying late Neoproterozoic to Cambrian Marwar Supergroup, made up of red-bed and evaporite sedimentary sequences (Pandit et al., 2001).

A volcaniclastic conglomerate lies at the base of MIS (Bhushan, 2000) and basal rhyolitic tuffs denote the initiation of basaltic and largely felsic flows of the first stage of the suite. This felsic extrusive episode was followed by the emplacement of granitic plutons and felsic dikes. Vertical to sub-vertical dolerite dikes crosscut all of the other components and thus mark the termination of magmatism. These mafic dikes intrude the Jalore Granite plutons south of Jodhpur and can be wide, up to 15 meters in extent (Figure 3-3). The mafic dike sequence near Jalore contains a relatively dense concentration of dikes with a general N-S trend. Many of the larger dikes form conspicuous ridges only when enclosed in a granite host and weather out as bouldery traces (Figure 3-3a). Fresh in-place outcrop is difficult to find, but we sampled 4 dikes exposed only in a granite quarry, most of which trend N-S. Sampling included a very thin N-S trending dikelet that is cut by a wider E-W trending dike that was also sampled. This dikelet is less than 2 cm wide, aphanitic and dark grey-black in color with obvious chilled margins (Figure 3-3b). There was no clear generative connection between this small dikelet and larger (nearby) N-S dikes; however, we cannot eliminate the possibility that it is rooted in a larger dike that was not exposed at this particular level in the quarry.

India magmatism can be compared with related Neoproterozoic igneous provinces on nearby cratons. Paleomagnetic data juxtapose the Seychelles alongside India, and northeastern Madagascar is also placed along the India margin based on temporal and geological similarities (Torsvik et al., 2001b; Ashwal et al., 2002). The sequence of rocks on Seychelles is distinctly similar to the Malani suite, and it is postulated that the geochemical signatures in the Seychelles are sourced from the Archean Banded Gneiss Complex near Rajasthan (Ashwal et al., 2002). The majority of Neoproterozoic granitoid and doleritic activity in the Seychelles falls within 755-748 Ma (Ashwal et al., 2002), with a span of reliable ages ranging from 808-703 Ma (Stephens et al., 1997). If the Seychelles suite of Neoproterozoic rocks is analogous to the Malani province, the dolerite dikes sampled in this study can be considered as equivalents to dolerite dikes of Seychelles. The Seychelles dikes are geochemically related to Seychelles granitoids (Ashwal et al., 2002), and a U-Pb zircon age at 750.2±2.5 Ma from one of those dikes (Takamaka dike) indicate they are nearly coeval with the felsic magmatic suite (Torsvik et al., 2001b). Slightly younger, but overlapping, ages (715-754 Ma) from the Daraina sequence in northern Madagascar are also correlated to the igneous activity in the Seychelles and India (Tucker et al., 1999).

Among the multitude of tectonic settings proposed for Malani magmatism, it is suggested (see Bhushan, 2000) that the first stage of associated basaltic and felsic flows is generated by a hot spot source or lithospheric thinning and melting at the base of the crust. However, both Madagascar and Seychelles have igneous activity from this time that is attributed to subduction of the Mozambique Ocean (Figure 3-1 inset; Handke et al., 1999; Torsvik et al., 2001b; Tucker et al., 2001; Ashwal et al., 2002). The MIS is often described as 'anorogenic magmatism' related either to crustal melting during extension or to an active hot spot (Bhushan, 2000; Sharma, 2004). Alternatively MIS magmatism can be interpreted in the context of an Andean-type active margin (Torsvik et al., 2001a; Torsvik et al., 2001b; Ashwal et al., 2002), closely related to the nearby, and coeval, arc activity observed in the Seychelles islands and northeastern Madagascar. The duration of magmatism and the source of igneous activity in the MIS, Seychelles and northeaster Madagascar are still questionable (Collins and Windley, 2002; Collins, 2006).

Previous Studies

Paleomagnetism

Numerous paleomagnetic studies have been performed on the felsic members of the MIS to determine the paleoposition of India at ca. 750 Ma (Table 1). Athavale et al. (1963) were the first to apply paleomagnetic tests to rhyolitic flows, and their results were similar to those obtained by Klootwijk (1975), but both studies lacked any detailed stability tests. Torsvik et al. (2001a) found a statistically positive fold test on felsic rocks from Malani. Folding of the Malani rocks occurred after eruption and prior to deposition of the flat-lying Cambrian Marwar supergroup, which constrains the age of the Malani pole to older than Cambrian. Late stage mafic dikes had not been subjected to paleomagnetic study prior to our work. No reversals or other field tests were found to further document the exact age of magnetism. The lack of additional positive field tests to fully constrain the age of magnetic acquisition has invoked some doubt in the primary nature of the Malani pole (Yoshida and Upreti, 2006).

Geochronology

Previous geochronologic results from Malani felsic volcanics span about 100 million years (Table 2). Crawford and Compston (1970) reported a pioneering Rb-Sr age of 730 ±10 Ma for rhyolites (re-calculated with a decay constant of 1.42 x10-11; Steiger and Jager, 1977). Later, Dhar et al. (1996) and Rathore et al. (1999) reported whole-rock Rb-Sr isochron ages ranging from 779 ±10 to 681 ±20 Ma for felsic volcanic rocks and granite plutons, emplaced during the first two stages of activity in the MIS (first and second stages, respectively). This wide distribution of dates is partially a result of studies of the so-called ultrapotassic rhyolites found near our sampling locality. The youngest Rb-Sr isochron age of 681 ±20 Ma (Rathore et al., 1999) comes from a solitary occurrence of the "ultrapotassic" rhyolite without any rock description that would ascertain whether high potassium is a primary igneous character or later alteration effect. Much younger apparent ages of 548 ±7 to 515 ±6 Ma were obtained from whole-rock 40Ar/39Ar data on Jalore granites. These apparent ages are interpreted as evidence for a thermal disturbance by Rathore et al. (1999) that may be related to the Kuungan or the Malagasy orogenies (Meert, 2003; Collins and Pisarevsky, 2005); however, the metamorphic grade of the rocks is incompatible with any significant thermal resetting (Ashwal et al., 2002). Torsvik et al. (2001a) cited precise U-Pb ages of 771 ±2 and 751 ±3 Ma for rhyolite magmatism in the MIS (Tucker, unpublished), but without analytical details and sample descriptions.

Methods

Paleomagnetic Sampling and Experiments

Samples were obtained in the field using a gasoline powered hand drill and oriented using magnetic and sun compasses. Readings from the sun compass were used to correct for the local declination and any magnetic interference from the outcrop. Twelve samples from Jalore Granite and about 50 samples from four mafic dikes were taken at three sites. Three of the granite samples include a small (width less than 2 cm) fined grained N-S trending dikelet (Figure 3-3b), which is crosscut by a 4-meter wide E-W trending mafic dike. The dikelet was sampled at 1.8 meters away from the larger dike, within a half-dike width distance. It was possible to drill only three cores, as boulders obstructed the remaining dikelet outcrop.

Samples were cut into standard sized specimens and stored in a magnetically shielded space in the University of Florida paleomagnetic laboratory. A few preliminary samples were stepwise treated thermally or with an alternating field to determine the best method of demagnetization. After analyzing the behavior of preliminary samples, a series of steps were chosen for either alternating field or thermal demagnetization. Alternating field demagnetization was applied in steps using a home-built AF-demagnetizer at fields up to 140 mT. Samples were also treated thermally in a stepwise manner, up to temperatures of 600˚C for ~60 minutes using an ASC-Scientific oven. Between each treatment, strong samples (generally mafic dikes) were measured on a Molspin Magnetometer and weaker samples (dikelets and granites) were measured on an ScT cryogenic magnetometer. Characteristic remanence components (ChRc) were calculated with least-square regression analysis implemented in the Super IAPD program (http://www.ngu.no/geophysics).

Rock Magnetic Experiments

The magnetic susceptibility of each sample was measured on an Agico SI-3B bridge before treatment. Curie temperature experiments were run on select powdered samples using a KLY-3S susceptibility bridge with a CS-3 heating unit. For this experiment, the susceptibility of a crushed sample is measured at increments during heating and cooling. The character of magnetic minerals in the sample can then be determined in detail based on the change in susceptibility with temperature. Isothermal Remanence Acquisition (IRM) studies were also performed using an ASC-IM30 impulse magnetizer to further characterize magnetic mineralogy.

Geochronology

Zircon was purified from one sample of rhyolitic tuff using a water table, heavy liquids and a magnetic separator. Available crystals were mounted in epoxy and polished to approximately half thickness. Cathodoluminescence (CL) images were obtained with a scanning electron microscope (Figure 3-4). U-Pb analyses were performed by secondary ion mass spectrometry (SIMS) using the CAMECA IMS 1270 instrument at the NORDSIM laboratory, Swedish Museum of Natural History, Stockholm (Table 3). The analytical method, data reduction, error propagation and assessment of the results are outlined in Whitehouse et al. (1999). The analyses were conducted with a spot size of ca. 20 μm, calibrating to the Geostandard of 91500 reference zircon with an age of 1065 Ma (Wiedenbeck et al., 1995). The error on the U-Pb ratio includes propagation of the error on the day-to-day calibration curve obtained by regular analysis of the reference zircon. A common Pb correction was applied using the 204Pb concentration and present-day isotopic composition (Stacey and Kramers, 1975). The ISOPLOT program (Ludwig, 1995) was used to regress and present the SIMS U-Pb data.

Results

Geochronologic Results

Zircon U-Pb geochronology was conducted on a sample of unfoliated rhyolitic tuff representing the first stage of volcanism in the MIS. The sample, Mis5/04, was collected close to Jodhpur (26º17.963’-72º58.357’) at site 3 of Torsvik et al. (2001a). The sample shows ca. 5 mm automorphic phenocrysts of quartz, plagioclase and K-feldspar in a microcrystalline devitrified groundmass of rose color. The sample contains few large (ca. 200 μm) prismatic zircon crystals. They show well-terminated pyramid tips and oscillatory zoning and contain common fluid and mineral inclusions. Their habit is typical for zircon formed in a volcanic/subvolcanic magmatic environment (Hoskin and Schaltegger, 2003). Sixteen analyses were made on 10 zircon crystals. Fourteen of them are concordant and define a concordia age of 771 ± 5 Ma (MSWD = 1.5; Figure 3-4). This age is interpreted as the timing of magmatic crystallization and deposition of the rhyolite tuff.

Rock Magnetic Results

Curie temperature runs on the mafic dike samples show a curve that is characteristic of magnetite, but with some alteration upon cooling (Figure 3-5b). Susceptibility is higher during heating than cooling, but Curie temperatures are similar and in the typical range of magnetite. The heating Curie temperature TcH is equal to 589.7˚C and the cooling Curie temperature TcC is equal to 588.3˚C. When subjected to temperatures up to 700˚C, mafic dikelets displayed substantial alteration and comparatively high susceptibility while cooling (Figure 3-5c). During demagnetization, samples are only heated to about 600˚C, so Curie temperature tests on the samples from the same dikelet were run up to only 600˚C and Curie curves showed far less alteration (Figure 3-5d). Thus alteration at high temperatures (>600˚C) is not an issue during demagnetization, and any alteration observed at lower temperatures is probably due to exsolution and conversion from Ti-magnetite to pure magnetite. Mafic dikes also have an Isothermal Remanance Magnetization (IRM) plot that is indicative of magnetite (Figure 3-5a). Samples saturate at ~0.3 tesla and their intensity remains constant at higher fields, up to the highest applied field of 2 tesla. Sample I434-28 is a mafic dikelet, and has an IRM curve also characteristic of magnetite, but with a lower absolute J value at saturation. Thermal demagnetization curves show unblocking at the characteristic magnetite temperature range of 550 to 570°C (Figure 3-6a).

Paleomagnetic Results

Table 4 lists paleomagnetic results from each site in this study. The mean direction resolved from four mafic dikes has a declination=358.8˚ and inclination=63.5˚ (k=91.2 and $\alpha 95$=9.7; Figure 3-8), after inverting one reverse polarity dike. The Virtual Geomagnetic Pole (VGP) calculated from the average direction of each dike falls at 70.2˚N, 70.1˚E (dp=12.1˚, dm=15.4˚). Figure 3-6 shows the typical demagnetization plots from two mafic dike sites. Most samples show a stable demagnetization trend, dependent on the treatment applied. Thermally treated samples unblock between 550 and 570˚ C and quickly lose over 50 percent of their intensity at this temperature range (Figure 3-6a). Samples treated with an alternating field lose intensity at a more gradual rate and do not generally unblock past greater than 80-85 percent of the original strength (Figure 3-6b). Most samples have a low temperature or low coercivity overprint that has no consistent direction, but is quickly removed. Jalore granite samples were taken with the intent to perform a baked contact test at site 34, but samples are dominated by multi-domain grains that have a strong, but unstable remanence, even with the application of low-temperature liquid nitrogen demagnetization. No stable directions were obtained from any granite samples, and intensity data also have no detectable trend with increasing distance from the large dike (up to 20 meters away).

Three samples were taken from the less than 2 cm wide dikelet pictured in figure 3-3b. The 4 meter wide dike at site 34 crosscuts this aphanitic dikelet at 1.8 meters away from the sampling location. Dikelet cores were taken at close to half-dike width away from the larger dike to observe the effects of dike emplacement on surrounding rocks. Unfortunately, due to limited outcrop, it was not possible to take a larger collection of dikelet samples. When treated with both alternating field and thermal demagnetization, samples display a high-temperature component that is antipodal to the three larger Malani dikes (Figure 3-7). Demagnetization trends of the dikelets include two distinct components and samples are weaker in intensity than the larger dikes. They show an increase in intensity at temperatures up to about 490˚C or fields to 40 mT (Figure 3-7). The low temperature and low coercivity component is identical to the mean direction from the normal polarity dikes with a declination=2.5, inclination=+57.5 (k=17.1 and α95=30.8), which is much steeper than the present-earth field in the region (inclination=43.4˚). The high temperature and high coercivity component has a reverse polarity with declination=195.3˚ and inclination=-59.7˚ (k=234.8 and α95=8.1).

Discussion

Significance of Paleomagnetic and Geochronologic Data

When results from Malani mafic dikes (this study, 4 sites) are combined with the trachyte and rhyolitic volcanics from Torsvik et al. (2001a; 9 sites) and Klootwijk (1975; 6 sites, Table 4), a mean direction is obtained with declination=001˚, inclination=63.0˚ (k=32.9, α95=5.9) and paleolatitude of 44.5˚. From this mean direction, a paleomagnetic pole for the MIS is placed at 67.8˚N, 72.5˚E (A95=8.8˚) after averaging VGPs from the 19 sites. The angular dispersion (S) of measured VGPs can be compared to the latitudinal variation in VGP angular dispersion as determined by Merrill et al. (1996) from IGRF90 (1990 International Geomagnetic Reference Field). VPG's from the Malani suite at paleolatitude 44.5˚ have an angular variance of 20.7˚

about the mean pole, calculated from the best estimate of angular variance for VGPs (equation 6.4.2 in McElhinny and McFadden, 1996). This value lies within the average VGP scatter that represents the time-averaged field about the earth's spin axis. The mean paleomagnetic pole for the MIS thus sufficiently averages secular variation, and such a scatter is generally inconsistent with a blanket remagnetization of the area.

The focus of this study is to reinforce the mean pole for India at ca. 770 Ma with paleomagnetic data from the last stage of MIS magmatism, and pair this with a robust age determination that was previously cited as a personal communication with unpublished and unavailable analytical data. The fortuitous sampling of a small dikelet with unique magnetic behavior provides even further, albeit tentative, support for the primary nature of the Malani pole. No reverse polarity direction or baked contact test was determined in previous work on the Malani suite. There are three possible interpretations for the magnetism observed in the dikelet: (1) the dikelet was emplaced in the same swarm as larger mafic dikes and experienced a true self-reversal, (2) the result is spurious and an unstable anomaly, or (3) the dikelet was emplaced aftere a field reversal and baked by the intrusion of subsequent mafic dikes, some thousands of years later and during a normal polarity field. Option (1) is very unlikely based on descriptions of observed natural self-reversing behavior. True self-reversal very rarely occurs in exsolved titanomagnetite compositions of basalt flows. The high Curie temperature phase (magnetite) aligns itself with the external field and influences the low temperature phase to the point of reversal (Merrill and McElhinny, 1983). This occurs in coarse, multi-domain grains during a slower cooling than that associated with aphanitic dikelet emplacement (Petherbridge, 1977; Merrill and McElhinny, 1983). The Malani dikelet has a high temperature direction that is reversed from the rest of the suite, which most likely formed parallel to the external, also reversed, field. This high temperature direction carries the reverse direction, thus even if this is a self-reversal, the reverse polarity direction in the dike is primary and only the low-temperature normal polarity could be an artifact of a true self-reversal. While sampling density is not sufficient to pass statistical reversal tests (i.e. McFadden and McElhinny, 1990, reversal test), all three samples from the dikelet demonstrated a normal overprint and antipodal directions upon heating.

In our opinion, option (3) best fits the results of the dikelet when compared to the larger dike intrusion. The dikelet was sampled at just within half dike-width away and thus still susceptible to partial baking by the large dike. Magnetic intensity increases in all samples as the normal polarity direction is removed (Figure 3-7b), which is typical behavior for the demagnetization of magnetic moments that are antipodal to the primary high temperature direction. We suggest that the dikelet was emplaced during a reversed polarity field and thousands of years later baked by a larger intrusion, resulting in a normal polarity overprint and a reverse primary direction. It is not uncommon for multiple dike intrusions to occur over enough time to include a field reversal. The Harohalli dike swarm in India (Pradhan et al., in press) and the Matachewan dikes in southern Canada (Irving and Naldrett, 1977; Halls, 1991; Halls and Zhang, 1998; Symons et al., 1994) are examples of dike swarms that were emplaced in multiple phases and include dual-polarity paleomagnetic results.

The Malani pole is cited as a representative pole for India during the late Neoproterozoic, yet some authors conclude that the lack of a decisive reversal or field test deems Malani paleomagnetic data untrustworthy (see Yoshida and Upreti, 2006 for example). However the results of our study not only add to the existing MIS paleomagnetic data set, but also provide additional evidence for a primary magnetization. The fold test provided by Torsvik et al. (2001a) is now augmented by evidence favoring a primary reverse TRM in the sequence overprinted by a normal-polarity magnetization in the mafic dikelet. Although this does not constitute a 'classic' backed contact test, the result is most easily explained as baking of the smaller dike. In addition, the Malani results do not overlap with younger poles from the Indian subcontinent nor is it consistent with a recent field overprint. The positive fold test determined by Torsvik et al. (2001) constraints the age of the pole to older than Cambrian and there are no paleomagnetic poles from the India craton within 750 to 560 Ma that have similar directions with the MIS that could represent a regional overprint. The Malani pole is also distinct from the more common overprints observed in Indian rocks in this region (Deccan and Rajmahal Traps) and from Carboniferous-Cretaceous paleomagnetic results observed in the Gondwana Supergroup and an analysis of post-Cretaceous paleomagnetic poles from India (Mallik et al., 1999; Acton, 1999). This even further attests the quality of this pole (Figure 3-8). The directions from Malani are also disparate from Carboniferous-Cretaceous paleomagnetic results observed in the Gondwana Supergroup and an analysis of post-Cretaceous paleomagnetic poles from India (Mallik et al., 1999; Acton, 1999).

The new zircon extrusion age of 771 ±5 Ma (Fig. 6) for a rhyolitic tuff places a robust age on the timing of the first stage of magmatism in the MIS. This age is consistent with the oldest available Rb-Sr isochron age of 779 ±10 Ma (Rathore et al., 1999), based on felsic volcanic rocks from widely spaced sampling sites. It is also consistent with the first of two 'personal communication' zircon dates at 771 ±2 and 751 ±3 Ma quoted by Torsvik et al. (2001a) for rhyolite magmatism in the first stage of MIS magmatism. These ages were determined with TIMS analysis at Washington University, St. Louis, on samples from sites 3 and 4 of Torsvik et al. (2001a), but analytical details were not given in the publication. Available Rb-Sr whole-rock geochronology (Crawford and Compston, 1970; Dhar et al., 1996; Rathore et al., 1999) defines a time span of nearly 100 m.y. (779 ±10 to 681 ±20 Ma), so one cannot rule out that the second and third stages of the magmatism are significantly younger than 771 ±5 Ma. Nevertheless, the consistency of paleomagnetic data for the different stages of magmatism argues for a comparatively short duration of activity. Paleomagnetic data from Malani dikes overlap with the ones from the 750.2 ±2.5 Ma Takamaka mafic dikes in Seychelles, if the two plates are juxtaposed together (Torsvik et al., 2001b). This provides further support for their correlation. In Figure 3-9, published site VGPs determined from the early stage of rhyolitic magmatism in the MIS (Klootwijk, 1975; Torsvik et al., 2001a) are compared to the VGPs derived from the third stage of magmatism of the suite (mafic dikes, this study). The mean direction from all VGPs is indicated (starred, Figure 3-9). We suggest that this indicates a relatively short eruptive history for the Malani suite, contradicting the over 100 million year span of apparent ages derived from Rb-Sr data (Rathore et al., 1999). Younger ages from Rb/Sr data can be accounted for by local disturbances or element mobility during minor episodes of metasomatism. Considering the nature and timing of magmatism in the Seychelles and India, the bulk of granitic and subsequent mafic magmatism in those regions was constrained to the interval from ca. 771 to 751 Ma.

Implications for the Configuration of Rodinia

It is postulated (Powell et al., 1993; Windley et al., 1994; Dalziel, 1997; Yoshida and Upreti, 2006) that a coherent East Gondwana existed from the Mesoproterozoic through the bulk of the Precambrian and until the Mesozoic breakup of Gondwana. This conclusion is largely based on paleomagnetic and detrital zircon data with high flexibility of interpretation and poor age control, as well as the alleged lack of evidence for appropriately aged oceanic sutures between eastern Gondwana cratons. Yoshida and Upreti (2006) discuss evidence for the Neoproterozoic juxtaposition of India and Australia-East Antarctica based on similarities in cratonic and orogenic detrital zircon and neodymium isotopic signatures. Yet the notion of a united East Gondwana through the Proterozoic and Cambrian is contradicted by high quality paleomagnetic data (Meert and Van der Voo, 1997; Meert, 2001; Torsvik et al., 2001a; Collins and Pisarevsky, 2005). Fitzsimons (2000) and Meert (2003) also review the evidence for appropriately aged mobile belts separating distinct segments of eastern Gondwana elements, which accounts for a later (Cambrian) ocean closure. In their discussion of the proximity of India and Australia-East Antarctica, Yoshida and Upreti (2006) argue that the paleomagnetic data used to constrain the possible separation of these continents do not include a well-constrained age and have been reset by later Pan-African events (ca. 530-510 Ma). We emphasize that this is not a valid argument because both the Malani pole reported in this paper and the highly reliable pole from the 755 ±3 Ma Mundine Well dike swarm in Australia (Wingate and Giddings, 2000) include necessary field and contact tests to argue against any resetting, and both are well-dated.

The paleolatitude of the 755 ±3 Ma Mundine Well dikes is 20.2˚ and this can be compared to the paleolatitude of the Malani dikes from our study (44.5˚), indicating a latitudinal separation of nearly 25° (Figure 3-10). It we use the Mundine pole as representative for East Gondwana at 750 Ma, it is necessary for India to be located along the paleoequator adjacent to East Antarctica according to its placement in the typically accepted Gondwana fit (deWit et al., 1988). Thus, the misfit between the latitude required by the Malani pole and India's "traditional" position is more than 45˚. It is possible that the southeast margin of India was located along the northwestern margin of Australia, but no geologic evidence such as oceanic sutures or similar-aged orogenic belts have been found to support this orientation. Younger-aged sutures between Gondwana components indicate a more complex Gondwana amalgamation as a series of distinct Pan-African orogenies that occurred between ca. 700 and 500 Ma (Fitzsimons, 2000; Meert, 2003; Collins and Pisarevsky, 2005). The East African Orogen (EAO) is the ca. 700-650 Ma result of collision between Madagascar, Somalia, Ethiopia and Arabian Nubian shield (collectively Azania block) and the Congo, Tanzania and Bangweulu block, first developed by Stern (1994) and has since been modified (Collins and Pisarevsky, 2005). The later Kuunga Orogen (Meert et al., 1995) places the final Gondwana assembly at about 550 Ma with the amalgamation of Australia-Antarctica with IMSLEK (India, northeastern Madagascar, Sri Lanka, East Antarctica, and the Kalahari craton) group. The Malagasy orogeny is also suggested to occur simultaneously with the Kuunga orogeny as the EAO constituents collided with southeastern India (Collins and Pisarevsky, 2005). These major Pan-African orogenies are congruent with a complex Gondwana assembly, and placing India alongside East Antarctica and Australia at 770 Ma fails to account for the existence of the considerably younger sutures.

Conclusions

The MIS provides the best paleomagnetic pole for the Indian subcontinent at approximately 771 Ma, with a combined pole of 67.8˚N, 72.5˚E (A95=8.8˚). Our study strengthens the case for primary magnetization of the MIS based on the primary reversed direction overprinted by a baked normal-polarity magnetization in a mafic dikelet. The now documented U-Pb zircon age of 771±5 Ma provides a more accurate and concordant lower age limit for Malani volcanism. When combined with geochronologic data from mafic dykes in the Seychelles (750.2±2.5, Torsvik et al., 2001b), our age determination also hints at a shorter duration of magmatic activity in the MIS than previously stated.

East Gondwana is considered by some authors to be a stable configuration from about 1.1 Ga until the Mesozoic breakup of Gondwana (Yoshida and Upreti, 2006). However, paleomagnetic data (Torsvik et al., 2001b, this study) place India and the Seychelles at much higher latitudes than coeval poles from Australia (Mundine dikes, Wingate and Giddings, 2000). Three robust paleomagnetic results (Mundine dykes, Malani Igneous Suite and Takamaka Dikes) argue strongly against an amalgamated East Gondwana at 750 Ma and therefore the younger Pan-African belts between these cratons are indicative of a Neoproterozoic-Cambrian suturing of eastern Gondwana. Thus, we argue that if paleomagnetism is to make any contribution to Neoproterozoic plate tectonic models, the Malani pole must be seriously considered in any geodynamic explanation for the assembly of Gondwana.

Acknowledgements: This work was supported by a grant (to JGM) from the National Science Foundation (EAR04-09101). The authors thank Jim Vogl and George Kamenov for help with relentless (unsuccessful) attempts to date the Malani dikes and we also thank Alan Collins and two anonymous reviewers for comments that greatly improved this manuscript. M. Whitehouse is thanked for operating the NORDSIM laboratory and controlling quality of U-Pb data.

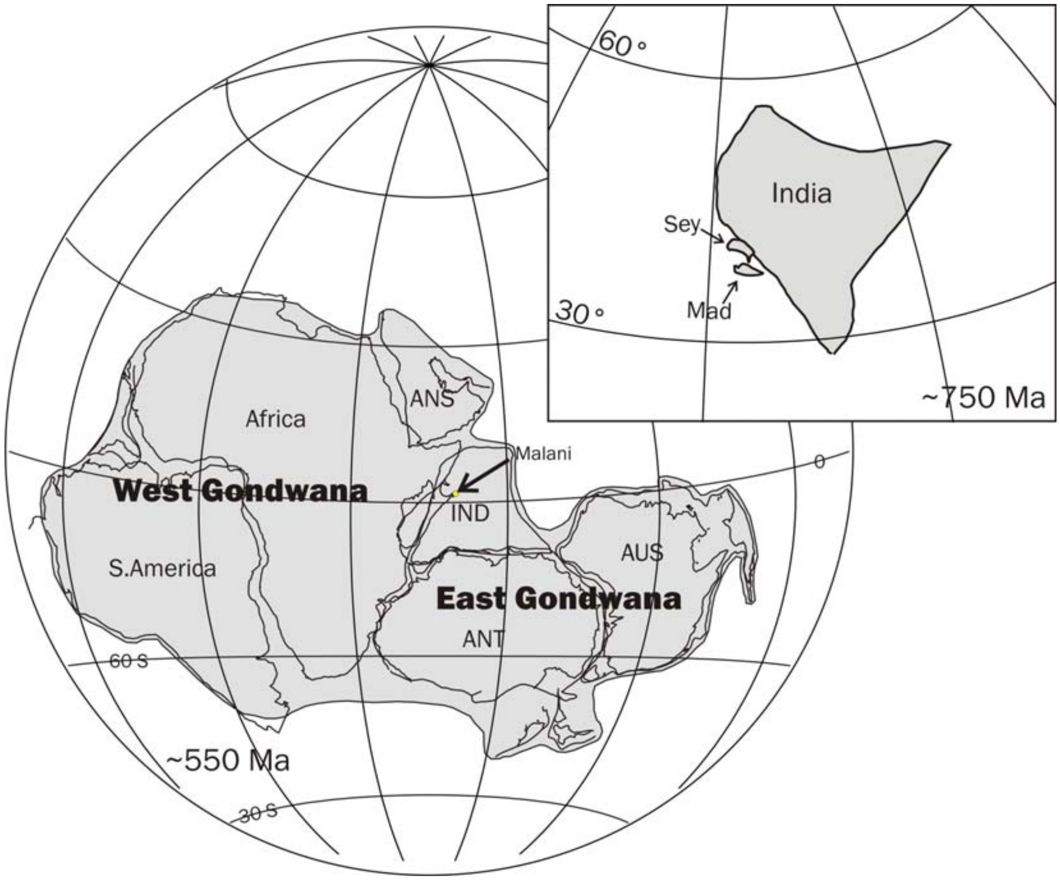

Figure 3-1. Typically accepted Gondwana fit for 560 Ma, taken from deWit et al., 1988 Reconstructions that use a Gondwana fit come from this model. Inset highlights the paleoposition of the Seychelles (Sey) and Madagascar (Mad) relative to India at 750 Ma, reconstructed using the Malani pole (Torsvik et al., 2001a) and the Seychelles euler pole of rotation (Torsvik et al., 2001b).

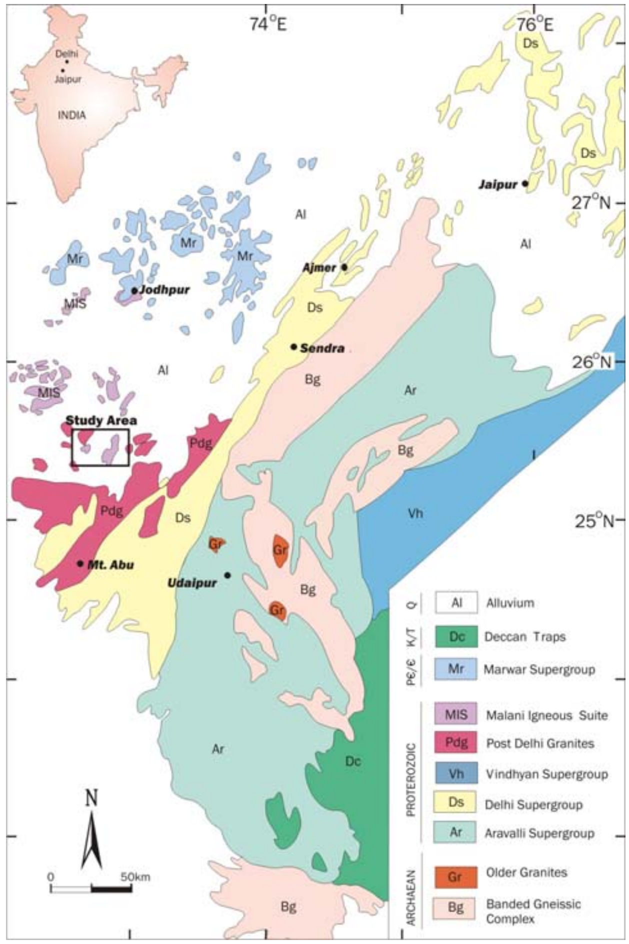

Figure 3-2. Map showing Precambrian stratigraphic units of the Aravalli Mountain Region in NW India with sampling area boxed (adapted from GSI publications).

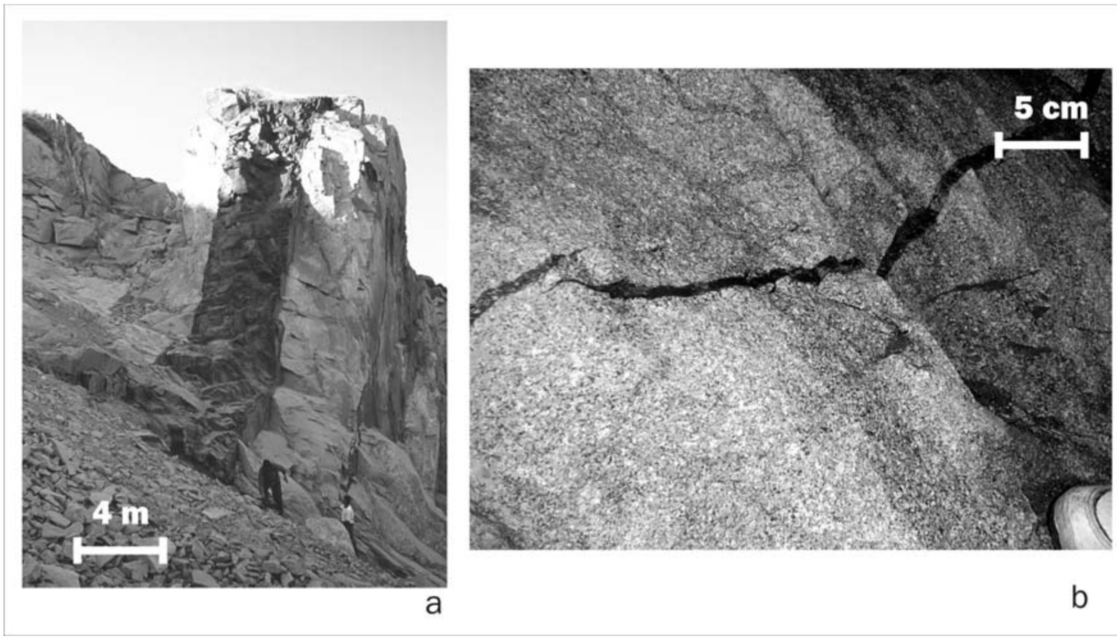

Figure 3-3. Field photos. (a) Photo of a large E-W trending dike at site I434 (b) Photo of 1 cm wide N-S trending mafic dikelet from site I434

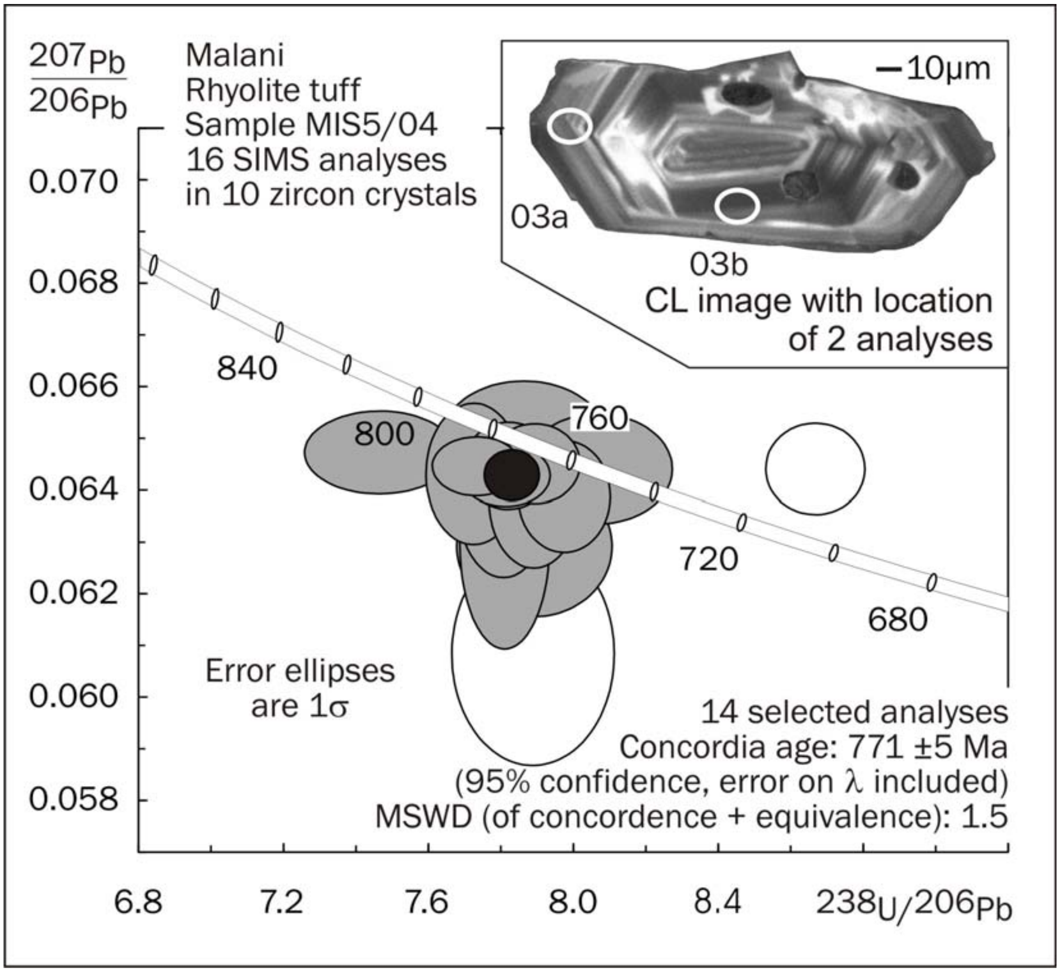

Figure 3-4. Inverse concordia diagram. Diagram shows U-Pb analyses of zircon and CL image of one zircon crystal from a rhyolitic tuff representing the first stage of magmatism in the Malani Igneous Suite. The concordia age of 771 ±5 Ma reflects magmatic crystallization of the rock.

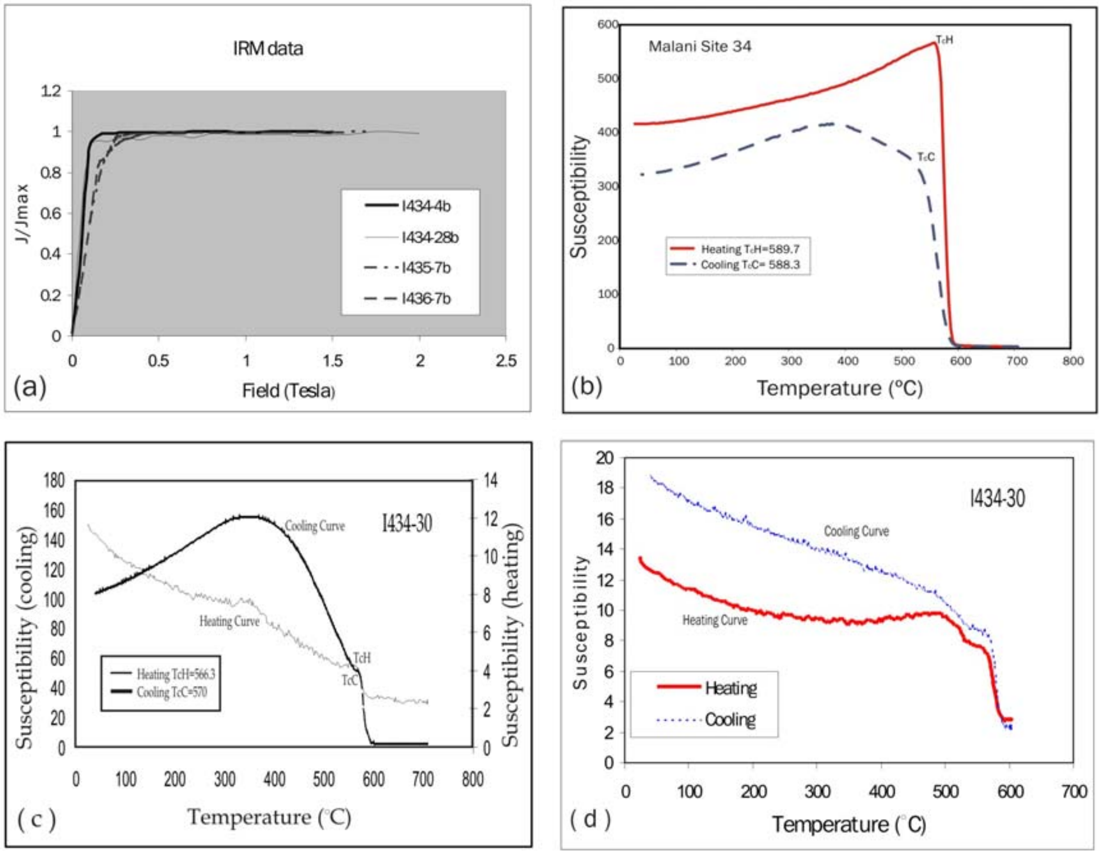

Figure 3-5. Magnetic characterization data. (a) Isothermal Remanence Magnetization (IRM) plots from four Malani samples. Sample I434-28 is a mafic dikelet. All samples saturate at about 0.3 tesla. (b) Curie temperature test of typical mafic dike sample from site I434. TcH indicates Curie temperature during heating, and TcC indicates Curie temperature during cooling, (c) Curie temperature test of a mafic dikelet. Tests were run up to 600˚C because of alteration at high temperatures.

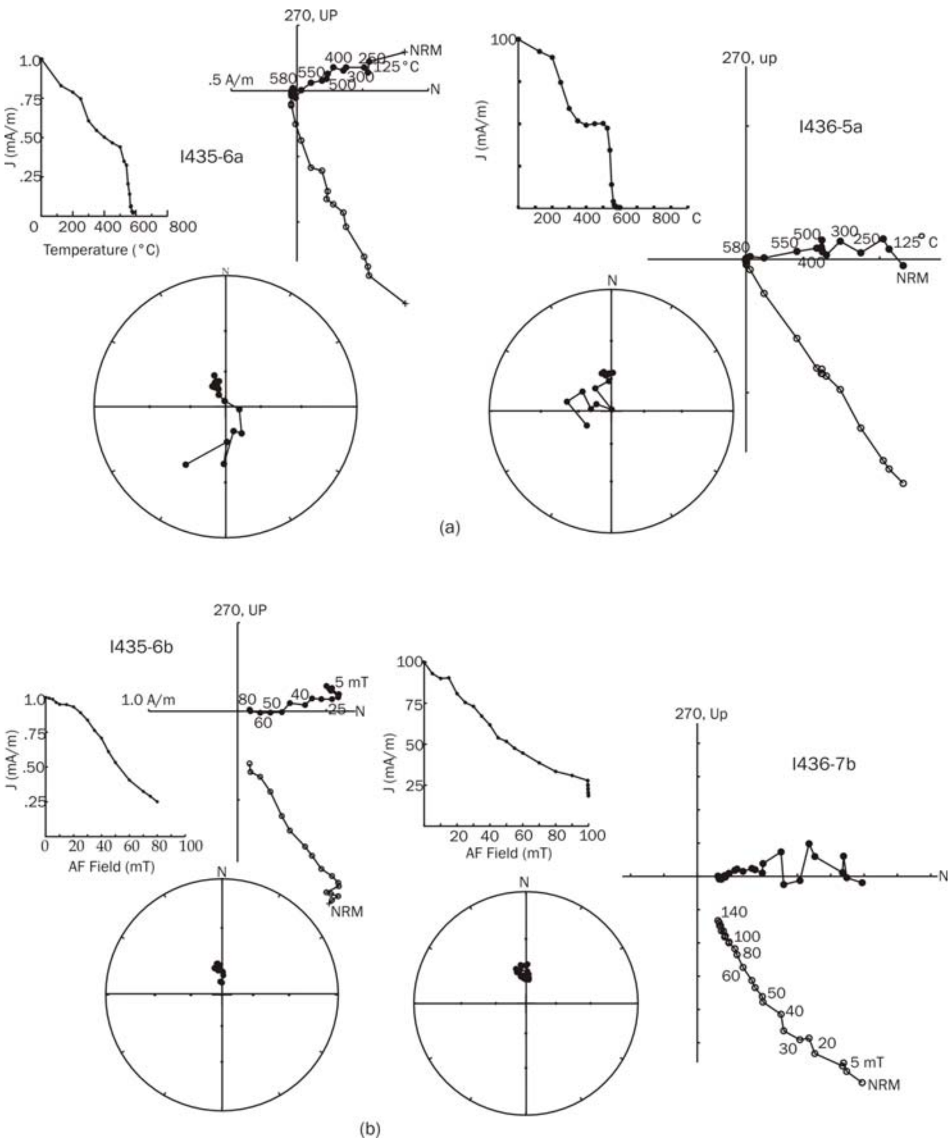

Figure 3-6. Demagnetization results from sites 35 and 36. (a) Thermal and (b) alternating field (AF) demagnetization results of mafic samples from sites 35 and 36. In stereoplots, closed circles represent positive inclinations. In Zijderveld diagrams closed (open) circles represent the horizontal (vertical) plane. NRM= Natural Remanent Magnetization. Thermal measurements are in ºC and AF measurements are in millitesla (mT).

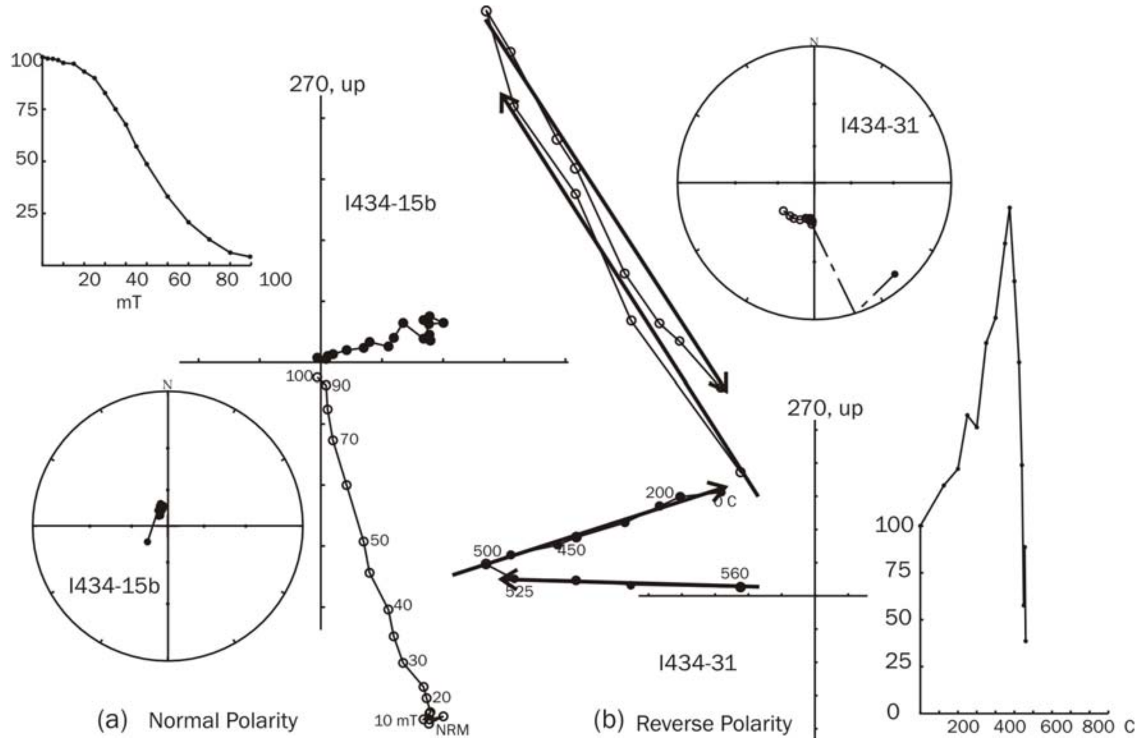

Figure 3-7. Demagnetization results from site 34. (a) Normal polarity sample subjected to AF demagnetization. (b) Reversed polarity dikelet sample with arrows pointing in direction from NRM to origin of both the overprint and reverse polarity vector. In stereoplots, closed circles represent positive inclinations. In Zijderveld diagrams closed (open) circles represent the horizontal (vertical) plane. NRM= Natural Remanent Magnetization. Thermal measurements are in ºC and AF measurements are in millitesla (mT).

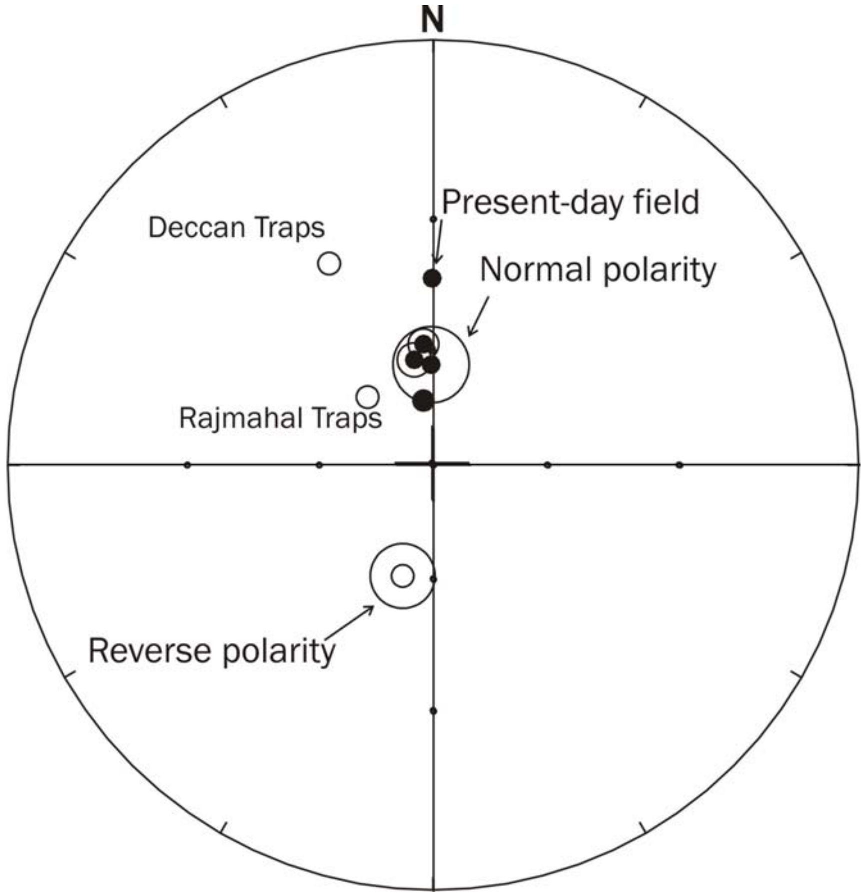

Figure 3-8. Stereoplot of individual site means, overall mean and reversed polarity mean with common India overprints from the Deccan Traps and Rajmahal Traps indicated

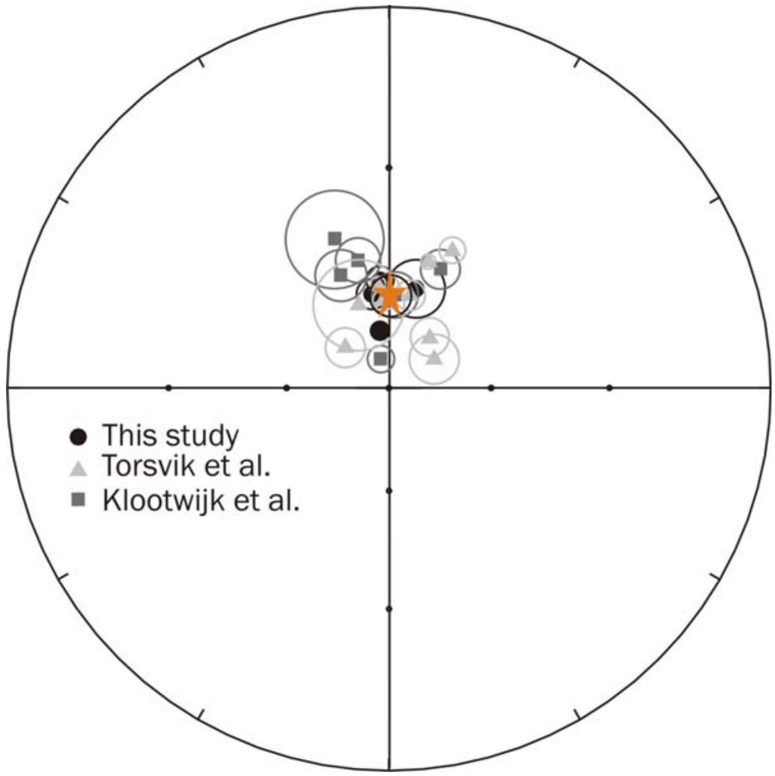

Figure 3-9. Stereoplot of VGPs from the three studies, averaged to the mean pole for the MIS. Circles are from mafic dikes (this study); triangles and squares are VGPs from each site of rhyolite and trachyite volcanics. Closed symbols represent positive inclinations.

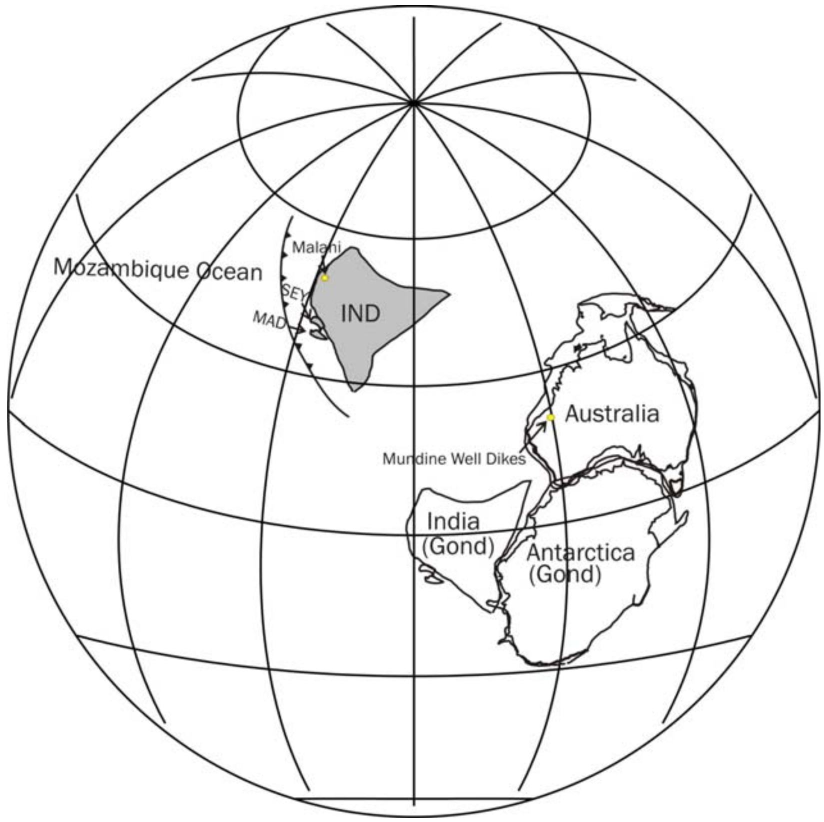

Figure 3-10. Reconstruction at 770 Ma of pertinent eastern Gondwana components. Grey India outline is plotted from the new mean Malani paleomagnetic pole, with the Seychelles euler rotation fit from Torsvik et al., (2001b) and Madagascar is placed according to the Gondwana fit. Australia is plotted according to the Mundine Wells dikes VGP, and Antarctica and India are placed in their Gondwana fit locations, in the Australia reference frame. There is >20º of latitudinal displacement between the Malani and Mundine Wells study sites.

Table 3-1. Summary of Paleomagnetic and Virtual Geomagnetic Poles

Pole Name	Age (Ma)	Pole latitude	Pole longitude	A95 or dp/dm[a]	dec[b]	inc[b]	α_{95}[c]	κ[d]	Reference
India									
Malani, aplite dike	750	74.6 N	49.8 E	16.2	352.5	60	16.2	18.6	Rao et al., 2003
Malani, rhyolite	745±10	80.5 N	43.5 E	8/11.5°	354.5	53.5	8		Klootwijk, 1975
Malani, felsic volcanics	751±3, 771±2	74.5 N	71.2 E	7.4/9.7°	359.5	60.4	6.4	29.9	Torsvik et al., 2001
Malani, rhyolite	740	78.0 N	45.0 E	11.0/15.0°	353	56	10		Athavale et al., 1963
Malani, mafic dikes, felsic volcanics	771±5*	70.2 N**	70.1 E	12.1/15.4°	358.8	63.5	9.7	91.2	this study
Seychelles									
Mahe dikes[IND]	750.2±2.5	79.8 N	78.6 E	9.9/14.9°	1.4	49.7	11.2		Torsvik et al., 2001
Australia									
Mundine Well dikes[IND]	755	41.47 N	130.92 E	4.1/4.1°	14.8	31.1	5		Wingate and Giddings, 2000

a: A95= cone of 95% confidence about the mean pole; dp/dm cone of 95% confidence about the paleomagnetic pole in the co-latitude direction (dp) and at a right angle to the co-latitude direction (dm), b: dec/inc= mean declination/ inclination, c: a95= circle of 95% confidence about the mean, d: k= kappa precision parameter, *U-Pb Age data reported in this study, samples are from site 3 of Torsvik et al., 2001, **Virtual Geomagnetic Pole (VGP) from four dikes

Table 3-2. Summary of geochronologic results

Site	Study	Method	Age (Ma)
Malani			
rhyolites	Crawford and Compston (1970)	Rb/Sr	730±10
rhyolites	Klootwijk (1975)	Rb/Sr	745±10
felsic volcanics	Rathore et al. (1996)	Rb/Sr isochron	779±10
ultrapotassic rhyolites	Rathore et al. (1999)	Rb/Sr isochron	681±20
Jalore granites	Rathore et al. (1999)	Rb/Sr isochron	727±8
peralkaline volcanics	Rathore et al. (1999)	Rb/Sr isochron	693±8
rhyolite	this study, site 3 of Torsvik et al., 2001a	U/Pb	771±5

Table 3-3: SIMS zircon U–Pb data on rhyolite tuff from Malani igneous suite

ID	U (ppm)	Th (ppm)	Pb (ppm)	$^{206}Pb/^{204}Pb$ [a]	$^{207}Pb/^{206}Pb$	±σ (%)	$^{207}Pb/^{235}U$	±σ (%)	$^{206}Pb/^{238}U$	±σ (%)	R [b]	$^{206}Pb/^{238}U$ [c] (Ma)	±σ	$^{206}Pb/^{238}U$ [d] (Ma)	±σ	Disc.[e] 2σ lim. (%)
MIS5/04: ryholite tuff [f]																
n1808-01a [g]	222	120	31	10257	0.06439	0.9	1.024	1.4	0.1154	1.0	0.75	704	7	703	7	
n1808-03a	414	202	64	17681	0.06449	0.8	1.127	1.3	0.1267	1.0	0.79	769	8	770	8	
n1808-03b	400	175	62	22494	0.06444	0.6	1.149	1.2	0.1294	1.0	0.87	784	8	785	8	
n1808-04a	85	63	14	5821	0.06372	1.5	1.126	1.8	0.1281	1.0	0.57	777	8	779	8	
n1808-05a	183	106	29	28736	0.06445	0.9	1.137	1.4	0.1279	1.0	0.77	776	8	777	8	
n1808-05b	196	149	33	6602	0.06430	1.4	1.148	1.8	0.1295	1.1	0.62	785	8	786	9	
n1808-05c	55	31	9	3629	0.06296	2.2	1.112	2.4	0.1281	1.0	0.43	777	8	779	8	
n1808-06a	149	113	24	6027	0.06385	1.1	1.104	1.5	0.1254	1.1	0.68	762	8	762	8	
n1808-06b	134	99	22	8903	0.06380	1.4	1.115	1.7	0.1268	1.0	0.60	769	8	771	8	
n1808-07a	401	316	67	13951	0.06426	0.6	1.134	1.2	0.1280	1.0	0.86	777	8	777	8	
n1816-01a	143	101	23	6033	0.06493	1.2	1.139	2.3	0.1272	1.9	0.85	772	14	772	15	
n1816-01b	197	154	32	14111	0.06377	1.0	1.119	2.2	0.1273	2.0	0.89	772	14	773	15	
n1816-02a [g]	46	24	7	3182	0.06076	2.4	1.062	3.0	0.1268	1.9	0.62	770	14	774	14	0.5
n1816-03a	88	57	14	13350	0.06288	1.4	1.099	2.3	0.1268	1.8	0.78	769	13	771	13	
n1816-03b	200	164	35	15016	0.06472	0.8	1.196	2.0	0.1340	1.8	0.91	811	14	812	14	
n1816-06a	138	54	20	10092	0.06440	1.1	1.101	2.0	0.1240	1.7	0.84	754	12	754	12	

a: Measured 206Pb/204Pb ratio, b: R correlation coefficient of errors in isotopic ratios, c: 204Pb corrected aged: 207Pb corrected age, c: age discordance at the closest approach of 2 s error ellipse to Concordia, f: coordinates of the sample: 26°17.963'-72°58.357', g: analysis not selected for calculation of concordia age.

Table 3-4: Paleomagnetic results

Site name	Lat/Long	n/N[a]	Declination	Inclination	Kappa (κ)[b]	α95[c]	VGP latitude[d]	VGP longitude[d]	dp, dm[e]
This study									
I434 (normal)	25.342˚N, 72.601˚E	23/27	351.4	72.6	129.55	2.7	56.9N	64.3E	4.3, 4.8
I434 (reverse)	25.342˚N, 72.601˚E	3/3	195.3	-59.7	234.79	8.1	70.2N	108.8E	9.2, 12.2
I435	25.341˚N, 72.601˚E	6/8	349.8	61.8	244.78	4.3	70.5N	49.8E	5.1, 6.7
I436	25.341˚N, 72.616˚E	9/9	355.4	58.2	256.88	3.8	75.9N	57.7E	4.1, 5.6
Combined mean		4 dikes	358.8	63.5	91.2	9.7	70.2N	70.1E	12.1, 15.4
Torsvik et al., 2001									
1	26.0˚N, 73.0˚E	5	038.6	70.6	188.9	5.6	49.7N	106.8E	8.4, 9.7
3	26.3˚N, 73.0˚E	13	017.2	51.8	678.2	1.6	73.8N	136.7E	1.5, 2.2
4	26.3˚N, 72.6˚E	13	312.8	72.3	51.7	5.8	44.5N	39.0E	9.1, 10.3
5	26.2˚N, 72.5˚E	6	356.2	64.1	511.1	3.0	70.1N	64.7E	3.8, 4.8
6	26.4˚N, 72.5˚E	11	024.7	46.7	178.9	3.4	68.0N	152.8E	2.8, 4.4
8	25.7˚N, 72.4˚E	16	354.0	59..4	322.0	2.1	74.6N	54.9E	2.4, 3.2
10	25.2˚N, 72.6˚E	4	339.9	64.0	51.6	12.9	63.9N	39.5E	16.4, 20.5
13	25.6˚N, 72.5˚E	5	057.5	74.0	109.0	7.3	38.0N	104.7E	11.9 13.2
14	25.7˚N, 72.4˚E	7	012.7	62.1	200.5	4.3	69.5N	99.6E	5.2, 6.7
Klootwijk et al., 1975									
RI-2	26.3˚N, 73.02˚E	6	003.9	62.5	133.0	6.5	72.2N	82.2E	7.9, 10.2
RI-3	26.3˚N, 73.02˚E	4	023.5	82.5	297.5	5.3	39.6N	80.6E	10.1, 10.3
RI-7	25.8˚N, 72.167˚E	4	340.0	45.0	55.0	12.5	72.1N	349.0E	10.0, 15.8
RI-10	25.8˚N, 72.167˚E	5	346.5	52.0	162.0	6.0	76.4N	15.4E	5.6, 8.2
RI-12	25.8˚N, 72.167˚E	3	337.0	54.5	316.0	7.0	68.2N	12.7E	7.0, 9.9
RI-13	25.67˚N, 73.15˚E	4	345.0	81.0	490.5	4.0	42.5N	67.1E	7.5, 7.7
Combined mean paleomagnetic pole		19 sites	001.0	63.0	32.9	5.9	67.8N	72.5.E	A95=8.8

a: n= samples used; N= samples collected, b: k= kappa precision parameter, c: a95= circle of 95% confidence about the mean, d: VGP latitude/longitude = virtual geomagnetic pole, e: dp,dm= cone of confidence along site latitude (dp) and orthogonal to site latitude (dm)

CHAPTER 4
CONCLUSION

The work included in this thesis presents glimpses into the Precambrian history of the Indian subcontinent. There are no reliable paleomagnetic poles for India between ca. 1050 and 770 Ma. Without further information, one cannot envision a convincing APWP for India between the low latitude Majhgawan pole and the mid-latitude Malani pole over the extended time span of 300 million years (Figure 4-1).

Paleomagnetic studies of the Vindhyanchal basin resolve similar poles to the Majhgawan kimberlite (Miller and Hargraves, 1994), but the age of the Upper Vindhyan sequence is very poorly constrained in the extant literature (see discussion in Chapter 2). The highly precise age of the Majhgawan kimberlite along with the similar paleomagnetic directions to the Vindhyan basin poles provided a catalyst for our group to conduct a detailed investigation on the age of sedimentation in the Upper Vindhyanchal basin (Malone et al., in revision). Previous constraints placed the upper age limit on Vindhyan sedimentation as Cambrian. Malone et al. resolved a paleomagnetic pole of 44ºN, 214ºE (A95= 4.3º), and the similarities in poles for these two units in India (Majhgawan and the Vindhyan) are consistent with detrital zircon analyses from the same study and are indicative of a much older limit for sedimentation in the basin (ca. 1050 Ma). Thus the Vindhyan pole can be added to the India APWP for the Mesoproterozoic, along with the 1192 Ma Harohalli dikes paleomagnetic poles (24.9° S, 258° E; A95=15°; Pradhan et al., 2008). Younger, pervasive overprints determined in Harohalli are tentatively assigned as Ediacaran on the basis of discordant zircon ages and coincidence of the directions with Gondwana and the ca. 600 Ma Dokhan Volcanics paleomagnetic pole from the Arabian-Nubien shield (Halls et al., 2007; Pradhan et al., 2008).

Chapter 3 focuses on the Neoproterozoic Malani Igneous Suite (MIS) and its implications for India relative to other eastern Gondwana components. The revised Malani pole places cratonic India at paleolatitude 44.5°, about 25° of latitudinal offset from the 755 Ma Mundine dikes pole in Australia. India is consequently offset 45° from its traditional Gondwana fit with Australia-Antarctica.

Multiple paleogeographic scenarios are posited for the various Gondwana components. Some suggest that East Gondwana amalgamated in the Mesoproterozoic and existed in the same configuration until Gondwana breakup in the Mesozoic (Windley et al., 1994; Piper, 2000; Yoshida and Upreti, 2006; Squire et al., 2006; Paulsen et al., 2007). This view is simplistic, and available data are more congruent with a complicated assembly of eastern Gondwana elements as a series of collisions occurring at the Precambrian-Cambrian boundary. The revised paleomagnetic pole for the MIS is in agreement with a much more complex assembly of eastern Gondwana.

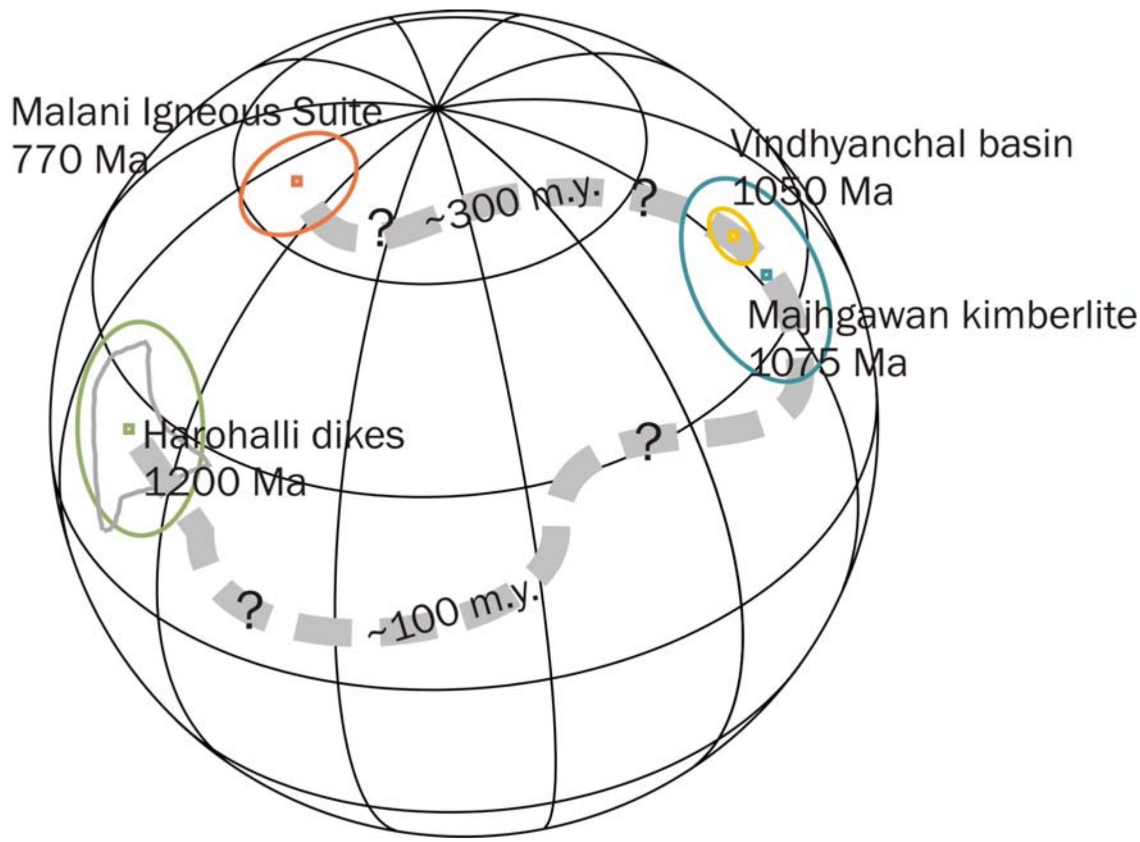

Figure 4-1: APWP for India with reliable Proterozoic poles. Poles are from Harohalli Dikes (Halls et al., 2007; Pradhan et al., 2008), the Majhgawan kimberlite (this study), the Vindhyanchal basin (Malone et al., in revision), and the Malani Igenous Suite (this study). The long gaps in the paleomagnetic record are highlighted, and the APWP between poles is dotted where data are nonexistent.

LIST OF REFERENCES

Acton, G.D., 1999. Apparent polar wander of India since the Cretaceous with implications for regional tectonics and True Polar Wander, Mem. Geological Society of India, 44, 129-175.

Ashwal, L.D., Demaiffe, D., Torsvik, T.H., 2002. Petrogenesis ofNeoproterozoic granitoids and related rocks from the Seychelles: evidence for the case of anAndean-type arc origin. Journal of Petrology 43, 45-83.

Athavale, R.N., Radhakrishnamurthy, C., Sahasrabudhe, P.W., 1963. Paleomagnetism of some Indian rocks, Geophysical Journal of the Royal Astronomical Society Soc., 7, 304-311.

Auden, J.B., 1933. Vindhyan sedimentation in Son Valley. Geolological Survey of India Memoirs 62, 141-250.

Boger, S.D., Carson, C.J., Fanning, C.M., Hergt, J.M., Wilson, C.J.L., Woodhead, J.D., 2002. Pan-African intraplate deformation in the northern Prince Charles Mountains, east Antarctica. Earth and Planetary Science Letters 195, 195-210.

Bond, G.C., Nickeson, P.A., Kominz, M.A., 1984. Breakup of a supercontinent between 625 and 555 Ma: new evidence and implications for continental histories. Earth and Planetary Science Letters 70, 325-345.

Bhushan, S.K., 2000. Malani Rhyolies- A Review. Gondwana Research 3, 65-77.

Chakrabarti, A., 1990. Traces and dubiotraces: examples from the so-called Late Proterozoic siliclastic rocks of the Vindhyan Supergroup around Maihar, India, Precambrian Research, 47, 141-153.

Chatterjee, A.K. and Rao, K.S., 1995. Majhgawan diamondiferous pipe, Madhya, Pradesh, India –A review, Journal of the Geological Society of India, 45, 175-189.

Collins, A.S., Windley, B.F., 2002. The tectonic evolution of central and northern Madagascar and its place in the final assembly of Gondwana. Journal of Geology 110, 325-340.

Collins, A.S., Pisarevsky, S.A., 2005. Amalgamating eastern Gondwana: The evolution of the Circum-Indian Orogens. Earth Science Reviews 71, 229-270.

Collins, A.S., 2006. Madagascar and the amalgamation of Central Gondwana. Gondwana Research (GR Focus) 9, 3-16.

Condon, D., Xhu, M.Y., Bowring, S., Wang, W., Yang, A.H., Jin, Y.G., 2005. U-Pb ages from the Neoproterozoic Doushantuo Formation, China. Science 308, 95-98.

Crawford, A.R., Compston, W., 1970. The age of the Vindhyan system of peninsular India. Quarterly. Journal of the Geological Society of London 125, 351-372.

Crawford, A.R., Compston, W., 1973. The age of the Cuddapah and Kurnool Systems, southern India. Journal of the Geolological Society of Australia 19, 453-464.

Dalziel, I.W.D., 1991. Pacific margins of Laurentia and East Antarctica as a conjugate rift pair: evidence and implications for an Eocambrian supercontinent. Geology 19, 598-601.

Dalziel, I.W.D., 1997. Neoproterozoic-Paleozoic geography and tectonics: Review, hypothesis and environmental speculation. Bulletin of the Geological Society of America 109, 16-42.

De, C., 2003. Possible organisms similar to Ediacaran forms from the Bhander Group, Vindhyan Supergroup, Late Neoproterozoic of India, Journal of Asian Earth Sciences, 21, 387-395.

De, C. 2006. Ediacara fossil assemblage in the Upper Vindhyans of Central India and its significance. Journal of Asian Earth Sciences, in press.

Deb, M., Thorpe, R., Kristic, D., 2002. Hindoli group of rocks in the eastern fringe of the Aravalli-Delhi orogenic belt-Archean secondary greenstone belt or Proterozoic supracrustals?, Gondwana Research, 5, 879-883

DeWit, M.J., Jeffrey, M., Bergh, H. and Nicolaysen, L., 1988. Geologic map of sectors of Gondwana reconstructed to their disposition at 150 Ma (1:10,000,000). American Association of Petroleum Geology, Tulsa, Ok.

Dhar, S., Frei, R., Kramers, J.D., Nägler, T.F., Kochhar, N., 1996. Sr, Pb and Nd isotope studies and their bearing on the petrogenesis of the Jalore and Siwana complexes, Rajasthan, India. Journal of the Geological Society of India 48, 151-160.

Evans, D.A.D, 2000. Stratgraphic, geochronological, and paleomagnetic constraints upon the Neoproterozoic climatic paradox, American Journal of Science, 300, 347-433.

Fitzsimons, I.C.W., 2000. A review of tectonic events in the East Antarctic Shield and their implications for Gondwana and earlier supercontinents. Journal of African Earth Science 31, 3-23

Gregory, L.G., Meert, J.G., Pandit, M., Pradhan, V.R., 2005. Paleomagnetic study of mafic dikes in India: Implications for continent assembly and dispersal, GSA Abstracts w/ Programs v.37, 303.

Haggerty, S.E., Birkett, T., 2004. Geological setting and chemistry of kimberlite clan rocks in the Dharwar Craton, India. Lithos 76, 535-549.

Halls, H.C., 1991. The Matachewan dike swarm, Canada: An early Proterozoic magnetic field reversal. Earth and Planetary Science Letters 105, 279-292.

Halls, H.C., Kumar, A., Srinivasan, R., Hamilton, M.A. (2007). Paleomagnetism and U-Pb geochronology of easterly trending dykes in the Dharwar craton, India: feldspar clouding, radiating dyke swarms and the position of India at 2.37 Ga. Precambrian Research 155, pp.47-68.

Halls, H.C., Zhang, B.X., 1998. Uplift structure of the southern Kapuskasing zone from 2.45 Ga dike swarm displacement. Geology 26, 67-70.

Handke, M.J., Tucker, R.D., Ashwal, L.D., 1999. Neoproterozoic continental arc magmatism in west-central Madagascar. Geology 27, 351-354.

Hoffman, P.F., Kaufman, A.J., Galen, P.H., Schrag, D.P., 1998. A Neoproterozoic Snowball Earth. Science, New Series 281, 1342-1346.

Hoffman, P.F., 1991. Did the breakout of Laurentia turn Gondwanaland inside out? Science 252, 1409-1412.

Hoskin, P.W.O., Schaltegger, U., 2003. The Composition of Zircon and Igneous and Metamorphic Petrogenesis in Zicon. Eds. Hanchar, J.M., Hoskin, P.W.O. Reviews in Mineralogy and Geochemistry 53, 27-62.

Irving, E., Naldrett, A.J., 1977. Paleomagnetism in Abitibi Greenstone Belt and Abitibi and Matachewan diabase dikes: Evidence of the Archean geomagnetic field. Journal of Geology 85, 157-176.

Jiang, G.Q., Sohl, L.E., Christie-Blick, N., 2003. Neoproterozoic stratigraphic comparison of the Lesser Himalaya (India) and Yangtze block (south China): Paleogeographic implications. Geology 31, 917-920.

Kaufman, A.J., Jiang, G., Christie-Blick, N., Banerjee, D.M., Rai, V., 2006. Stable isotope record of the terminal Neoproterozoic Krol platform in the Lesser Himlayas of northern India. Precambrian Research 145, 156-185.

Kirschvink, J.L., 1980. The least square line and plane and the analysis of paleomagnetic data, Geophys. Journal of the Royal Astronomical Society, 62, 699-718.

Klootwijk, C.T., 1973. Paleomagnetism of Upper Bhander Sandstones from Central India and implications for a tentative Cambrian Gondwanaland reconstruction, Tectonophysics, 18, 123-145.

Klootwijk, C.T., 1975. A note on the palaeomagnetism of the late Precambrian Malani rhyolites near Jodhpus; Indian Journal of Geophysics 41, 189-200.

Klootwijk, C.T., Nazirullah, R., de Jong, K.A., 1986. Paleomagnetic constraints on formation of the Mianwali reentrant, Trans-Indus and western Salt Range, Pakistan, Earth and Planetary Science Letters, 80, 394-414.

Kumar, A. and Gopalan, 1992. Precise Rb-Sr ages of South Indian Kimberlites and Central Indian Lamporites, Intr. Round Table Conference on Diamond Exploration and Mining, p. 21.

Kumar, S. and Srivastava, P. 2003. Carbonaceous megafossils from the Neoproterozoic Bhander Group, central India, Journal of the Paleontological Society of India, 48, 139-154.

Kumar, B., Das Sharma, S., Sreenivas, B., Dayal, A.M., Rao, M.N., Dubey, N. and Chawla, B.R., 2002. Carbon, oxygen and strontium isotope geochemistry of Proterozoic carbonate rocks of the Vindhyan basin, central India, Precambrian Research 113, 43-63.

Li, X.I., Bogdanova, S.V., Collins, A.S., Davidson, A., De Waele, B., Ernst, R.E., Fitzsimons, I.C.W., Fuck, R.A., Gladkochub, D.P., Jacobs, J., Karlstrom, K.E., Lu, S., Natapov, L.M., Pease, V., Pisarevsky, S.A., Thrane, K., Vernikovsky, V., 2008. Assembly, configuration, and break-up history of Rodinia: A synthesis. Precambrian Research 160, 179-210.

Ludwig, K.R. (1995) Isoplot, version 2.82: a plotting and regression program for Radiogenic isotope data. 45 p. U.S. Geological Survey, Open-file report 91-445.

Mallik, S.B., Piper, J.D.A., Das, A.K., Bandyopadhyay, G. and Sherwood, G.J., 1999. Paleomagnetic and rock magnetic studies in the Gondwana Supergroup (Carboniferous-Cretaceous), NE India. Memoirs of the Geological Society of India 44, 87-116

Malone, S.J., Meert, J.G., Pandit, M.K., Kamenov, G.D., Pradhan, V.R., Tamrat, E. Paleomagnetism of the Upper Vindhyan Sequence, Son Valley and Rajasthan, India: A possible 500 Ma downward revision in the age of the Purana Basins? Journal of Geology, in revision.

Mathur, S.M., 1962. Geology of the Panna diamond deposits, Geol. Surv. India Records, 87, 787-818.

Mathur, S.M., 1981. A revision of stratigraphy of the Vindhyan Supergroup in the Son Valley, Mirzapur District, Uttar Pradesh, Geological Society of India Miscellaneous Publications, 19, 78-85

McElhinny, M.W., Cowley, J.A., Edwards, D.J., 1978. Paleomagnetism of some rocks from peninsular India and Kashmir. Tectonophysics, 50, 41-54.

McFadden, P., McElhinny, M.W., 1990. Classification of the reversal test in paleomagnetism. Geophysical Journal International 103, 725-729.

McMenamin, M.A.S., McMenamin, D.L.S., 1990. The Emergence of Animals; The Cambrian Breakthrough. Columbia University Press, New York. 217 pp.

Meert, J.G., Van der Voo, R., Ayub, S., 1995. Paleomagnetic investigation of the Gagwe lavas and Mbozi Complex, Tanzania and the assembly of Gondwana. Precambrian Research 74, 225-244.

Meert, J.G., Van der Voo, R., 1997. The assembly of Gondwana 800-550 Ma. Journal of Geodynamics 23, 223-235.

Meert, J.G., 2001. Growing Gondwana and rethinking Rodinia. Gondwana Research 4, 279 288.

Meert, J.G., 2003. A synopsis of events related to the assembly of eastern Gondwana. Tectonophysics 362, 1-40.

Meert, J.G., Torsvik, T.H., 2003. The making and unmaking of a supercontinent: Rodinia revisited. Tectonophysics 375, 261-288.

Meert, J.G. and Lieberman, B.S., 2008. The Neoproterozoic assembly of Gondwana and its relationship to the Ediacaran-Cambrian radiation, Gondwana Research, doi:10.1016/j.gr2007.06.007.

Merril, R.T., McElhinny, M.W., 1983. The Earth's Magnetic Field: Its History, Origin and Planetary Perspective. Int. Geophys. Series 32, Academic Press, 401 p.

Merril, R.T., McElhinny, M.W., McFadden, P.L., 1996. The Magnetic Field of the Earth: Paleomagnetism, the Core, and the Deep Mantle. Int. Geophys. Series 63, Academic Press, 531 p.

Miller, K.C. and Hargraves, R.B., 1994. Paleomagnetism of some Indian Kimberlites and lamporites, Precambrian Research, 69, 259-267.

Moores, E.M., 1991. Southwest U.S.-East Antarctica (SWEAT) connection: a hypothesis. Geology 19, 425-428.

Mukherjee, A., Rao, K.S., Chatterjee, A.K., 1997. Chemistry of Phlogopite Megacrysts in Majhgawan Dimondiferous Pipe, Panna, Madhya Pradesh, Journal of the Geological Society of India, 49, 203-206.

Owada, M., Osanai, Y., Toyoshima, T., Tsunogae, T., Hokada, T., Crowe, W.A., Kagami, H., 2003. Early Proterozoic tectonothermal events in the Napier complex, East Antarctica: Implications for the formation of East Gondwana. Gondwana Research 6, 231-240.

Pandit, M.K., Shekhawat, L.S., Ferreira, V.P., Sial, A.N., Bohra, S.K., 1999. Trondhjemite and Granodiorite Assemblages from West of Barmer: Probable Basement for Malani Magmatism in Western India. Journal of the Geological Society of India 53, 89-96.

Pandit, M.K., Sial, A.N., Jamrani, S.S., Ferreira, V.P., 2001. Carbon isotopic profiles across the Bilara Group rocks of trans-Aravalli Marwar Supergroup in western India: Implications for Neoproterozoic – Cambrian transition. Gondwana Research 4, 387-394.

Pareek, H.S., 1981. Petrochemistry and petrogenesis of the Malani igneous suite, India summary. Geological. Society of Americal Bulletin 1 (92), 67-70.

Paul, D.K., 1979. Isotopic composition of strontium in Indian kimberlites, Geochimica et Cosmochimica Acta, 43, 389-394.

Paul, D.K., Potts, P.J., Gibson, I.L., Harris, P.G., 1975. Rare-earth abundances in Indian kimberlite, Earth and Planetary Science Letters, 25, 151-158.

Paulsen, T.S., Encarnaci´on, J., Grunow, A.M., Watkeys, M., 2007. New age constraints for a short pulse in Ross orogen deformation triggered by East-West Gondwana suturing, Gondwana Research, doi: 10.1016/j.gr.2007.05.011.

Petherbridge, J., 1977. A magnetic coupling occurring in partial self-reversal of magnetism and its association with increased magnetic viscosity in basalts. Geophysical Journal of the Royal Astronomical Society 50, 395.

Piper, J.D.A., 1976. Palaeomagnetic evidence for a Proterozoic supercontinent. Philosophical Transactions of the Royal Society of London A280, 469-490.

Piper, J.D.A., 2000. The Neoproterozoic Supercontinent: Rodinia or Palaeopangaea? Earth and Planetary Science Letters 176, 131-146.

Pisarevsky, S.A., Wingate, T.D., Powell, C.McA., Johnson, S., Evans, D.A.D., 2003. Models of Rodinia assembly and fragmentation, in Yoshida, M., Windley, B.F., Dasgupta, S. (eds) 2003. Proterozoic East Gondwana: Supercontinent Assembly and Breakup. Geological Society, London, Special Publcations, 206, 35-55.

Powell, C.McA., McElhinny, M.W., Meert, J.G., Park, J.K., 1993. Paleomagnetic constraints on timing of the Neoproterozoic breakup of Rodinia and the Cambrian formation of Gondwana. Geology 21, 889-892.

Powell, C.M., Pisarevsky, S.A., 2002. Late Neoproterozoic assembly of East Gondwana. Geology 30, 3-6.

Pradhan, V.R., Pandit, M.K., Meert, J.G., in press. A cautionary note on the age of the paleomagnetic pole obtained from the Harohalli dyke swarms, Dharwar Croton, Southern India, in Indian Dykes, ed. Srivastava, S.K., Sivaji, Ch., Rao, N.V.C.

Prasad, B., 1984. Geology, Sedimentation and Palaeogeography of the Vindhyan Supergroup, southeastern Rajasthan, Memoirs of the Geolological Survey of India, 116, Part 2, pp. 1-58.

Rai, V., Shukla, M., Gautam, R., Vibhuti, R., Shukla, M., and Gautam, R., 1997. Discovery of carbonaceous megafossils (Chuaria-Tawuia assemblage) from the Neoproterozoic Vindhyan succession (Rewa Group), Allahabad - Rewa area, India, Current Science, 73, 783-788

Rasmussen, B., Bose, P.K., Sakar, S., Banerjee, S., Fletcher, I.R., McNaughton, N.J., 2002. 1.6 Ga U-Pb zircon age for the Chorhat Sandstone, lower Vindhyan, India: Possible implications for early evolution of animals, Geology, 30, 103-106.

Rathore, S.S., Venkatesan, T.R., Srivastava, R.K., 1999. Rb-Sr Isotope Dating of Neoproterozoic (Malani Group) Magmatism from Southwest Rajasthan, India:Evidence of Younger Pan African Thermal Event by 40Ar-39Ar Studies. Gondwana Research 2, 271-281.

Rau, T.K. and Soni, M.K., 2003. Diamondiferous Vindhyan conglomerates and their provenance; a critical study, Indian Mineralogist, 37, 22-30.

Ray, J.S., 2006. Age of the Vindhyan Supergroup: A review of recent findings. Journal of Earth Systems and Science 115, 149-160.

Ray, J.S., Martin, M.W., Veizer, J., Bowring, S.A., 2002. U-Pb zircon dating and Sr isotope systematics of the Vindhyan Supergroup, India, Geology, 30, 131-134.

Ray, J.S., Veizer, J., Davis, W.J., 2003. C, O, Sr and Pb isotope systematics of carbonatesequences of the Vindhyan Supergroup, India: age, diagenesis, correlations and implications for global events, Precambrian Research, 121, 103-140.

Renne, P.R., Swisher, C.C., Deino, A.L., Karner, D.B., Owens, T.L., DePaolo, D.J., 1998. Intercalibration of standards, absolute ages and uncertainties in 40Ar/39Ar dating, Chemical Geology (Isot. Geosci. Section), 145,117-152.

Sarangi, S., Gopalan, K., Kumar, S., 2004. Pb-Pb age of earliest megascopic, eukaryotic alga bearing Rohtas Formation, Vindhyan Supergroup., India: implications for Precambrian atmospheric oxygen evolution. Precambrian Research 132, 107-121.

Sharma, K.K., 2004. The Neoproterozoic Malani magmatism of the northwestern Indian shield: Implications for crust-building processes. Proceedings of the Indian Academy of Science (Earth and Planetary Science) 113, 795-807.

Skinner, E.M.W., Marsh, J.S., 2004. Distinct kimberlite pipe classes with contrasting eruption processes. Lithos 76, 183-200.

Smith, C.B.,1992. The age of the Majhgawan Pipe, India, Scott Smith Petrology, p.9.

Squire, R.J., Campbell, I.H., Allen, C.M., Wilson, C.J.L., 2006. Did the Transgondwanan Supermountain trigger the explosive radiation of animals on Earth? Earth and Planetary Science Letters.

Srivastava, A.P. and Rajagopalan, G., 1988. F-T ages of Vindhyan glauconitic sandstone beds exposed around Rawabhata area, Rajasthan, Journal of the Geological Society of India, 32, 527 529.

Stacey, J.S., and Kramers, J.D., 1975. Approximation of terrestrial lead isotope evolution by a two-stage model. Earth and Planetary Science Letters 26, 207–221.

Steiger, R.N. and Jager, E., 1977. Subcommission on Geochronology: convention on the use of decay constants in geo- and cosmochronology, Earth and Planetary Science Letters, 36, 359-362.

Steiner, M., 1997. Chuaria circularis WALCOTT 1899 - "megasphaeromorph acritarch" or prokaryotic colony?, Acta Universitatis Carolinae Geologica 40, p. 645-665.

Stephens, W.E., Jemielita, R.A., Davis, D., 1997. Evidence for ca. 750 Ma intra-plate extensional tectonics from granite magmatism on the Seychelles: new geochronological data and implications for Rodinia reconstructions and fragmentation. Terra Nova 9, 166.

Stern, R.J., 1994. Arc assembly and continental collision in the Neoproterozoic East African orogen: implications for the consolidation of Gondwanaland. Annual Reviews of Earth and Planetary Science 22, 225-244.

Symons, D.T.A., Lewchuk, M.T., Dunlop, D.J., Costanzoalvarez, V., Halls, H.C., Bates, M.P., Palmer, H.C., Vandall, T.A., 1994. Synopsis of paleomagnetic studies in the Kapuskasing structural zone. Canadian Journal of Earth Science 31, 1206-1217.

Torsvik, T.H., Carter, L.M., Ashwal, L.D., Bhushan, S.K., Pandit, M.K., Jamtveit, B., 2001a. Rodinia refined or obscured: palaeomagnetism of the Malani igneous suite (NW India). Precambrian Research 108, 319-333.

Torsvik T.H., Ashwal, L.D., Tucker, R.D., Eide, E.A., 2001b. Neoproterozoic geochronology and palaeogeography of the Seychelles microcontinent: the India link. Precambrian Reseach 110, 47-59.

Tucker, R.D., Ashwal, L.D., Hamilton, M.A., Torsvik, T.H., Carter, L.M., 1999. Neoproterozoic silicic magmatism in northern Madagascar, Seychelles and NW India: clues to neoproterozoic supercontinent formation and dispersal. Geological Society of America Abstracts Program 31, A317 (abstract).

Tucker, R.D., Ashwal, L.D., Torsvik, T.H., 2001. U-Pb geochronology of Seychelles granitoids: a Neoproterozoic continental arc fragment. Earth and Planetary Science Letters 187, 27-38.

Venkatachala, B.S., Sharma, M., Shukla, M, 1996. Age and life of the Vindhyans- Facts and conjectures, Memoirs of the Geological Society of India, 36, 137-165.

Vinogradov, A.P., Tugarinov, A.I., Zhikov, C.I., Stanikova, N.I., Bibikova, E.V., Khorre, K., 1964. Geochonology of Indian Precambrian, Report 22nd International Geological Congress New Delhi, 10, 553-567.

Weil, A.B., Van der Voo, R., MacNiocaill, C., Meert, J.G., 1998. The Proterozoic supercontinent Rodinia: Paleomagnetically derived reconstruction for 1100 to 800 Ma. Earth and Planetary Science Lettters 154, 13-24.

Whitehouse, M.J., Kamber, B.S., and Moorbath, S., 1999. Age significance of U–Th–Pb zircon data from early Archaean rocks of west Greenland – a reassessment based on combined ion-microprobe and imaging studies. Chemical Geology 160, 201-224.

Wiedenbeck, M., Allé, P., Corfu, F., Griffin, W.L., Meier, M., Oberli, F., Von Quadt, A., Roddick, J.C., and Spiegel, W., 1995. Three natural zircon standards for U-Th Pb, Lu-Hf, trace element and REE analyses. Geostandards Newsletter 19, 1–23.

Windley, B.F., Razafiniparany, A., Razakamanana, T., Ackermund, D., 1994. Tectonic framework of the Precambrian of Madagascar and its Gondwana connections: a review and reappraisal. Geol. Rundsch. 83, 642-659.

Wingate, M.T.D., Giddings, J.W., 2000. Age and palaeomagnetism of the Mundine Well dyke swarm, Western Australia: implications for an Australia-Laurentia connection at 550 Ma. Precambrian Research 100, 335-357.

Yoshida, M., Upreti, B.N., 2006. Neoproterozoic India within East Gondwana: Constraints from recent geochronologic data from Himalaya. Gondwana Research 10, 349-356.

Zhang, S.H., Jiang, G.Q., Zhang, J.M., Song, B., Kennedy, M.J., Christie-Blick, N., 2005. U-Pb sensitive high-resolution ion microprobe ages from the Doushantuo Formation in south China: Constraints on Late Neoproterozoic glaciations. Geology 33, 473-476.

BIOGRAPHICAL SKETCH

Less than a month ago, I was in remote Mongolia, teetering precariously on an outcrop of volcanic rocks formed over 500 million years ago, using a hand-held diamond bit drill to extract samples that will elucidate the complex details of Central Asia's geologic history. I am an explorer, but not in the traditional sense. I delve into the earth's elusive past, where oceans have closed and opened, mountains have uplifted and eroded away, and continents have met in vast landmasses only to break up and drift apart.

My father sparked my interest in science. He is a biologist with a doctorate in entomology and I was always enamored with his careful descriptions of the natural world and his enthusiasm for learning. A class titled "The Biology of Fireflies" ultimately swayed me into the pursuit of science. The professor of the course, Dr. Lloyd, spent the past thirty years vigorously investigating the atypical subject of fireflies. Dr. Lloyd demonstrated that with scientific scrutiny even the seemingly insignificant firefly becomes magnificently intricate. I sought to find a subject equally interesting and fortuitously happened upon earth sciences. Every single day of my first class in geology challenged my intellect, and I started working on research by the end of the semester.

Undergraduate research allowed me to complete a combined bachelors and masters degree, focusing on the ancient locations of continents using paleomagnetism and geochronology. I developed a passion for tectonics and structural geology and decided to apply for a doctorate degree. I will continue my graduate carreer at Oxford University next Fall, 2008.